

**SOLUTION OF THE NON-LINEAR THIRD ORDER PARTIAL DIFFERENTIAL
EQUATION OF A STEADY HYDROMAGNETIC FLOW THROUGH A
CHANNEL WITH PARALLEL STATIONARY POROUS PLATES**

BY

KANDIE JOSEPH KIPCHIRCHIR

**A THESIS SUBMITTED IN PARTIAL FULFILLMENT OF THE
REQUIREMENTS FOR THE DEGREE OF DOCTOR OF PHILOSOPHY IN
APPLIED MATHEMATICS IN THE SCHOOL OF SCIENCE**

UNIVERSITY OF ELDORET, KENYA

AUGUST, 2018

DECLARATION

Declaration by the candidate

This thesis is my original work and has not been submitted for any academic award in any institution; and shall not be reproduced in part or full, or in any format without the prior permission from the author and/or University of Eldoret.

KANDIE JOSEPH KIPCHIRCHIR

SC/PHD/M/011/11

Signature..... Date

Declaration by the Supervisors

This thesis has been submitted with our approval as University Supervisors.

1. PROF. JACOB K. BITOK

Department of Mathematics and Computer Science

University of Eldoret, Kenya

Signature Date

2. PROF. ALFRED W. MANYONGE

Department of Pure and Applied Mathematics

Maseno University, Kenya

Signature Date

3. DR. JULIUS S. MAREMWA

Department of Mathematics and Computer Science

University of Eldoret, Kenya

Signature Date

DEDICATION

To my mum Tapkigen, my wife Elizabeth and my children Cheruiyot, Kipkogei, Kiplimo
and Kipruto

ABSTRACT

This thesis deals with the solution of the non-linear third order partial differential equation of a steady hydromagnetic laminar flow of a conducting viscous incompressible fluid through a channel with two parallel porous plates. The two plates are stationary and there is magnetic field moving at right angle to the electric field. Due to the porous nature of the plates, the fluid is withdrawn through both walls of the channel at the same rate. The specific equations governing the flow are discussed, transformed using dimensionless techniques into a third order partial differential equation, simplified using Taylor's series expansion and solved by the method of regular perturbation. Expressions for the velocity components and temperature profiles are discussed and represented in form of tables and graphs plotted by use of MATLAB programming software. The velocity profiles parallel (axial) and normal (radial) to the plates as well as the temperature distribution on the fluid are investigated. The results indicate that the radial velocity decreases with increase in Reynolds number while the axial velocity is zero at the walls and increases to the maximum at the centre line depicting the normal free flow velocity of the stream when there is no magnetic field in the fluid flow. The velocity of the fluid decreases with increase in Hartmann number. The temperature of the fluid decreases when Prandtl number increases and Eckert number decreases. This means that when viscous forces increases in the flow the thermal conductivity becomes negligible and thus thermal energy surpasses the kinetic energy of the fluid. The study has its application in hydromagnetic devices where the interaction between velocities profiles, magnetic and electric fields are utilized in the design of various machines, for instance removal of pollutants from plant discharge stream by absorption.

TABLE OF CONTENTS

DECLARATION	ii
DEDICATION	iii
ABSTRACT.....	iv
TABLE OF CONTENTS.....	v
LIST OF TABLES	vii
LIST OF FIGURES	viii
LIST OF SYMBOLS	ix
ACKNOWLEDGMENT.....	xii
CHAPTER ONE	1
INTRODUCTION	1
1.1 Background of the problem	1
1.2 Definitions of basic concepts	2
1.2.1 Two dimensional flow	2
1.2.2 Steady flow	2
1.2.3 Incompressible flow	3
1.2.4 Laminar flow.....	3
1.2.5 Viscosity	3
1.2.6 Inertia forces	4
1.2.7 Reynolds number, <i>Re</i>	4
1.2.8 Eckert number, <i>Ec</i>	5
1.2.9 Prandtl number, <i>Pr</i>	5
1.2.10 Hartmann number, <i>M</i>	5
1.3 Governing equations	5
1.3.1 Equation of continuity.....	6
1.3.2 Momentum equation	7
1.3.3 Equation of conservation of energy	10
1.3.4 Ohm's Law.....	11
1.3.5 Maxwell's equations	12
1.4 Statement of the problem	13
1.5 Objectives of the study.....	14

1.6 Significance of the study.....	14
CHAPTER TWO	15
LITERATURE REVIEW	15
2.1 Introduction.....	15
2.2 Literature review	15
CHAPTER THREE	21
METHODOLOGY	21
3.1 Introduction.....	21
3.2 Formulation of the problem	21
3.2.1 Assumptions and approximations	23
3.2.2 Conditions at the porous plate.....	23
3.2.3 Non-dimensionalization	24
3.3 Perturbation Theory	29
CHAPTER FOUR.....	37
RESULTS AND DISCUSSION	37
4.1 Introduction.....	37
4.2 Results.....	37
4.2.1 Radial velocity, \mathbf{vr}	37
4.2.2 Axial velocity, \mathbf{va}	41
4.2.3 Temperature	46
4.3 Discussion.....	47
CHAPTER FIVE	49
CONCLUSION AND RECOMMENDATION.....	49
5.1 Conclusion	49
5.2 Recommendations.....	50
Attia, H. A. (1997). Transient MHD Flow and Heat transfer between Two Parallel Plates with Temperature dependent Viscosity. <i>Mechanic Resource Community</i> , Vol 26 115-121.	52
APPENDICES	55
APPENDIX I: Data for radial velocity, axial velocity and temperature.....	55
APPENDIX II: MATLAB Program	64

LIST OF TABLES

1. Table A1: Radial velocity, v_r for $M = 0$ and varying R	51
2. Table A2: Radial velocity for $R = 0.001$ and varying M	52
3. Table A3: Values of Radial velocity when varying both M and R	53
4. Table A4: Values of Radial velocity for very small R and large M	54
5. Table A5: Axial velocity values for $R=0.001$ and varying M	55
6. Table A6: Axial velocity for values of Constant $M=0$ and varying R (0.01, 10, and 20)	56
7. Table A7: Axial velocity Values for small R and large M	57
8. Table A8: Comparison of Radial and Axial velocities	58
9. Table A9: Temperature Values for $Pr(2, 1, 0.5)$ and $Ec(1, 3, 0.5)$	59

LIST OF FIGURES

1. Figure 3.1: The physical configuration of the problem	20
2. Figure 4.1: Radial velocity profiles as a function of η for constant $M=0$ and varying R	35
3. Figure 4.2: Radial velocity profiles as a function of η for constant $R=0.001$ and varying M	36
4. Figure 4.3: Graph of radial velocity profiles as a function of η for the range of $R(1-6,)$ and $M(3,6,9)$	37
5. Figure 4.4: Graph of radial velocity profiles as a function of η for small R and large M	38
6. Figure 4.5: Graph of radial velocity profiles as a function of η for constant $R=0.001$ and varying M (0.01, 10, 20)	39
7. Figure 4.6: Axial velocity profiles as a function of η for constant $M=0$ and varying $R(0.01,10,20)$	40
8. Figure 4.7: Graph of axial velocity profiles as a function of η for large R and small M	41
9. Figure 4.8: Graph of radial and axial velocity profiles as a function of η for $R=0.1$ and $M=1$	42
10. Figure 4.9: Graph of temperature profiles as a function of η for $Pr(2, 1, 0.5)$ and $Ec(1, 3, 0.5)$	43

LIST OF SYMBOLS

\vec{B} Magnetic induction

F_x Body force along x-direction

F_y Body force along y-direction

C_p Specific heat capacity at constant pressure

\vec{D} Electric displacement

e Unit electric charge

\vec{E} Electric field intensity

Ec Eckert number

\vec{F} Force

g Acceleration due to gravity

\vec{H} Magnetic field intensity

h Characteristic length parallel to y – axis

\vec{j} Current density

K Thermal conductivity

L Characteristic length parallel to x-axis

M Hartmann number

P Pressure of the fluid

Pr Prandtl number

\vec{q} Velocity

R Suction Reynolds number

Re Reynolds number

T Dimensional temperature

u_0 Characteristic velocity

$\frac{D}{Dt}$ Material derivative or substantial derivative

ρ Fluid density

ρ_e Electric charge density

ν Kinematic viscosity

μ Coefficient of viscosity (dynamic viscosity)

μ_ϵ Magnetic permeability

τ Shear stress

σ Electric conductivity

η Dimensionless y-coordinate variable

$\vec{\nabla}$ Gradient operator

∇^2 Laplacian operator

ACKNOWLEDGMENT

I thank the Almighty God for His grace that has enabled me to carry out this study. My sincere appreciation goes to my Supervisors: Prof. Jacob Bitok, Prof. Alfred Manyonge and Dr. Julius Maremwa who worked tirelessly with me, giving valuable comments and positive suggestions that have inspired me and enhanced the quality of this study.

I would also like to thank the entire department of Mathematics and Computer Science of University of Eldoret particularly the Head, Dr. Betty Korir for her constant encouragement and administrative support during my study. My special regards also goes to my family members especially my wife for her prayers, support and kind, caring, loving and patiently encouraging me finish my studies. Finally to my classmates Nyamai, Limo, Bundotich, Wahome, Saina and all those who directly or indirectly contributed to the success of this work, may the glory of God richly bless you All.

CHAPTER ONE

INTRODUCTION

1.1 Background of the problem

The magnetohydrodynamic as a word was first used by Hannes Alfvén in 1942 for which he received a Nobel Prize in physics in 1970, Kimeu et al (2014). The term ‘magneto hydrodynamic’ usually abbreviated MHD and is derived from magneto meaning magnetic field, hydro meaning liquid and dynamic meaning movement. Hydrodynamics is therefore the study of fluid flow and the forces that causes the flow without the electromagnetic field while hydromagnetic involves the interaction of electrically conducting fluid and electromagnetic fields, for instance, Plasma, salt solution and mercury. When these fluids move past a magnetic field, there arises an interaction between the flow field and the magnetic field which exerts a force on the fluid due to the induced currents thus it affects the original magnetic field. The forces generated in this way are of the same order of magnitude as the hydrodynamic forces and are taken into account when considering the fluid flow. These forces are known as body forces and acts on the fluid. Examples of these forces are gravitational and electromagnetic forces. The dynamic effect of the fluid flow system can therefore be described in terms of flow variables such as velocity, density and pressure. For steady flow, these variables remains constant at all stages of the fluid flow.

The hydromagnetic fluid flow between parallel porous plates is a classical problem in fluid dynamics and is known as Hartmann flow. The porous plate is one with pores (void

space) on the plate. The solution to this problem has many applications in MHD power generators in that it generates electricity from thermal or kinetic energy by the use of conducting fluid as the electrical conductor; in electrostatic precipitation for air purification; in oil reservoir engineering; in lubrication of porous bearings; in porous walled flow reactors and in polymer technology among others. Therefore, there is need to study the two dimensional hydromagnetic flow of a steady incompressible fluid between two parallel porous plates.

1.2 Definitions of basic concepts

1.2.1 Two dimensional flow

It is the fluid flow in which all flows occur in a set of parallel planes with no flow normal to them, and the flow is identical in each of these parallel planes. Mathematically, it is written as

$u = f_1(x, y)$, $v = f_2(x, y)$ where x and y are the coordinate axes and u and v are their corresponding velocities respectively.

1.2.2 Steady flow

It is a type of flow in which the fluid properties (velocity, pressure or density etc) can change from point to point in the control volume but remains the same at any fixed point during the whole process, which the fluid flow remains constant throughout the flow region even though time is varying. During a steady flow process the total amount of mass contained within a control volume does not change with time, hence obeys the conservation of mass principle which states that the total amount entering a control volume is equal to the total amount of mass leaving it.

1.2.3 Incompressible flow

It is the flow where by each travelling fluid element changes its density negligibly or not at all. That is, a flow in which the material density is constant within a fluid parcel (an infinitesimal volume) that moves with the flow velocity. Mathematically, $\rho = \text{constant}$.

1.2.4 Laminar flow

It is the movement of the fluid flow which does not suffer from disturbance. The fluid particles move along well defined paths or stream lines which are straight and parallel. The particles move in layers gliding smoothly over the adjacent layer. The fluids that exhibit this flow are irrotational and the streamlines never loops back on themselves thus there is no mixing between the different fluid layers as well as there is no slip condition at the boundary. These flows remain orderly in continuous motion along the plate until a critical distance is reached or the Reynolds number attain a critical value after which a small disturbance in the flow begin to be amplified which characterize the end of laminar boundary layer.

1.2.5 Viscosity

It is the property of the fluid which determines its resistance to shear stress between the layers of the fluid. It is a measure of internal fluid friction which causes resistance to the fluid flow. A fluid at rest cannot resist shearing forces and if such forces act on a fluid which is in contact with a solid boundary, the fluid will flow over the boundary in a such a way that the particles immediately in contact with the boundary have the same velocity as boundary while successive layers of the fluid parallel to the boundary move with increasing velocities. Shear stresses opposing the relative motion of these layers are set up, their magnitude depending on the velocity gradient from layer to layer. For fluid

obeying Newton's law of viscosity and taking u as the velocity of the fluid in the x -direction at a distance y from the boundary, shear stress in the x -direction is mathematically written as

$$\tau = \mu \frac{du}{dy} \quad (1.1)$$

where $\frac{du}{dy}$ is the velocity gradient. All fluids which obey this relation are known as Newtonian fluids. These are the forces that relates to the internal friction in the fluid flow. The particles due to these forces are in continuous steady motion in a straight line parallel to the axis and at a fixed point the motion always remains constant. The types of fluid flow where these forces are involved are called viscous flow. They are thick or sticky flows in which the fluid particles are considered to be aggregates of molecules that move along streamlines so that at any point they are always constant, for instant honey.

1.2.6 Inertia forces

These are forces that cause the acceleration of the fluid particles in motion to be zero. They resist change in the velocity of an object and are in the opposite direction of an applied force.

1.2.7 Reynolds number, Re

It is a dimensionless number and is the ratio of inertia forces to viscous forces.

Mathematically expressed as

$$Re = \frac{\rho u L}{\mu} = \frac{u L}{\nu} \quad (1.2)$$

If for any flow, this number is small, the inertia forces are negligible and the flow is predominated by the viscous forces otherwise inertia forces predominate and the effect of

viscosity are negligible. The number is used to find the velocity, density, viscosity and length of the fluid

1.2.8 Eckert number, E_c

It is the ratio of kinetic energy to thermal energy usually written as

$$E_c = \frac{u^2}{c_p \Delta T} = \frac{u^2}{c_p (T_2 - T_1)} \quad (1.3)$$

This dimensionless number is a measure of kinetic energy of the flow relative to the enthalpy difference across the boundary layer and used in continuum mechanics.

1.2.9 Prandtl number, P_r

It is the ratio of viscous forces to thermal conductivity written as

$$P_r = \frac{\mu c_p}{k} = \frac{\rho \nu c_p}{k} \quad (1.4)$$

It is a dimensionless number approximating the ratio of the momentum diffusion to thermal diffusivity. Prandtl number provides a measure of relative effectiveness of momentum and energy transport by diffusion in the velocity and thermal boundary layers respectively.

1.2.10 Hartmann number, M

It is the ratio of electromagnetic forces to the viscous forces, expressed as

$$M = Bh \left(\frac{\sigma}{\nu \rho} \right)^{\frac{1}{2}} = Bh \sqrt{\frac{\sigma}{\mu}} \quad (1.5)$$

1.3 Governing equations

The general governing equations for hydromagnetic flow are:

1.3.1 Equation of continuity

It is derived from the conservation of mass which states that the mass flow into the infinitesimal volume must be equal to the mass flow out of the volume. The conservation laws are Lagrangian in nature, which is they apply to fixed systems (particles) while Eulerian system, which is appropriate to fluid flow utilizes the particle derivative:

$$\frac{D}{Dt} = \frac{\partial}{\partial t} + (\vec{V} \cdot \nabla) \quad (1.6)$$

Which is a formidable expression and is equivalent to

$$\frac{Dm}{Dt} = \frac{D(\rho v)}{Dt} = 0 = \rho \frac{Dv}{Dt} + v \frac{D\rho}{Dt} \quad (1.7)$$

The term $\frac{Dv}{Dt}$ is related to fluid velocity by noticing that the total dilatation or normal-strain rate is equal to the rate of volume (v) increase of the particle of unit volume:

$$\epsilon_{xx} + \epsilon_{yy} = \frac{1}{V} \frac{Dv}{Dt} \quad (1.8)$$

Further, it can be substituted for the strain rates from kinematic relations to get

$$\epsilon_{xx} + \epsilon_{yy} = \frac{\partial u}{\partial x} + \frac{\partial v}{\partial y} = \nabla \cdot \vec{V} \quad (1.9)$$

Combining (1.7) to (1.9) to eliminate V , the equation of continuity for fluids in its most common general form is obtained, that is

$$\frac{\partial \rho}{\partial t} + \frac{\partial(\rho u)}{\partial x} + \frac{\partial(\rho v)}{\partial y} = 0 \quad (1.10)$$

Since a steady incompressible flow is considered, then ρ is a constant and therefore

$\frac{\partial \rho}{\partial t} = 0$, hence equation (1.10) reduces to

$$\frac{\partial u}{\partial x} + \frac{\partial v}{\partial y} = \nabla \cdot \vec{V} = 0 \quad (1.11)$$

1.3.2 Momentum equation

The equation of conservation of momentum states that the time rate of change of momentum of a body is equal to the external force applied to the body. This external force includes surface forces and body forces. It is derived from Newton's second law of motion which requires that the sum of all forces acting on the control volume be equal to the rate of increase of the fluid momentum within the control volume.

$$\mathbf{F}(\text{external}) = m\mathbf{a} \quad (1.12)$$

External forces acting on the control volume are twofold:

1) *Body forces*-these are the forces proportional to the control volume, which apply to the entire mass of the fluid element e.g. gravitational, electric, magnetic and/ or centrifugal fields.

2) *Surface forces*-these are proportional to the area of the control volume and results from the stresses on the sides of the element, such as static pressure and viscous stresses. They arise from the action of one body to another across the surface of the contact between them.

$$\text{Therefore, } m\mathbf{a} = \text{Body forces} + \text{Surface forces} \quad (1.13)$$

$$\text{But } m = \rho dx dy \quad (1.14)$$

Thus from Navier-Stokes equations, the x- and y-momentum respectively is given as

$$\rho \left(u \frac{\partial u}{\partial x} + v \frac{\partial u}{\partial y} \right) = F_x + \frac{\partial}{\partial x} \delta_{xx} + \frac{\partial}{\partial y} \tau_{yx} \quad (1.15)$$

and

$$\rho \left(u \frac{\partial v}{\partial x} + v \frac{\partial v}{\partial y} \right) = F_y + \frac{\partial}{\partial y} \delta_{yy} + \frac{\partial}{\partial x} \tau_{xy} \quad (1.16)$$

The stresses are related to the velocity components in the form (Mohanty, 2006)

$$\delta_{xx} = -p + 2\mu \frac{\partial u}{\partial x}, \delta_{yy} = -p + 2\mu \frac{\partial v}{\partial y} \quad \text{and} \quad \tau_{xy} = \mu \left(\frac{\partial u}{\partial y} + \frac{\partial v}{\partial x} \right) \quad (1.17)$$

Substituting (1.17) in (1.15) we have

$$\rho \left(u \frac{\partial u}{\partial x} + v \frac{\partial u}{\partial y} \right) = F_x + \frac{\partial}{\partial x} \left(-p + 2\mu \frac{\partial u}{\partial x} \right) + \frac{\partial}{\partial y} \left(\mu \left(\frac{\partial u}{\partial y} + \frac{\partial v}{\partial x} \right) \right) \quad (1.18a)$$

$$\rho \left(u \frac{\partial u}{\partial x} + v \frac{\partial u}{\partial y} \right) = F_x - \frac{\partial p}{\partial x} + 2\mu \frac{\partial^2 u}{\partial x^2} + \mu \frac{\partial^2 u}{\partial y^2} + \mu \frac{\partial^2 v}{\partial y \partial x} \quad (1.18b)$$

$$\rho \left(u \frac{\partial u}{\partial x} + v \frac{\partial u}{\partial y} \right) = F_x - \frac{\partial p}{\partial x} + \mu \frac{\partial^2 u}{\partial x^2} + \mu \frac{\partial^2 u}{\partial x^2} + \mu \frac{\partial^2 u}{\partial y^2} + \mu \frac{\partial}{\partial x} \left(\frac{\partial v}{\partial y} \right) \quad (1.18c)$$

$$\rho \left(u \frac{\partial u}{\partial x} + v \frac{\partial u}{\partial y} \right) = F_x - \frac{\partial p}{\partial x} + \mu \left(\frac{\partial^2 u}{\partial x^2} + \frac{\partial^2 u}{\partial y^2} \right) + \mu \frac{\partial}{\partial x} \left(\frac{\partial u}{\partial x} + \frac{\partial v}{\partial y} \right) \quad (1.18d)$$

Simplifying (1.18d) using (1.11), the x-momentum equation (1.15) becomes

$$\rho \left(u \frac{\partial u}{\partial x} + v \frac{\partial u}{\partial y} \right) = F_x - \frac{\partial p}{\partial x} + \mu \left(\frac{\partial^2 u}{\partial x^2} + \frac{\partial^2 u}{\partial y^2} \right) \quad (1.19)$$

Similarly the y-momentum equation (1.16) becomes

$$\rho \left(u \frac{\partial v}{\partial x} + v \frac{\partial v}{\partial y} \right) = F_y - \frac{\partial p}{\partial y} + \mu \left(\frac{\partial^2 v}{\partial x^2} + \frac{\partial^2 v}{\partial y^2} \right) \quad (1.20)$$

Dividing (1.19) by ρ and taking into account the external body force for an Ohmic conductor which is due to electromagnetic force, $\vec{F} = \vec{j} \times \vec{B}$ and that the force of gravity along x-axis is zero, then the x-component of equation (1.20) becomes

$$u \frac{\partial u}{\partial x} + v \frac{\partial u}{\partial y} = -\frac{1}{\rho} \frac{\partial p}{\partial x} + \frac{\mu}{\rho} \left(\frac{\partial^2 u}{\partial x^2} + \frac{\partial^2 u}{\partial y^2} \right) + \frac{\vec{j} \times \vec{B}}{\rho} \quad (1.21)$$

The current density \vec{j} is proportional to electric field \vec{E} that is $\vec{j} = \sigma \vec{E}$, and that

$$\vec{E} = \vec{u} \times \vec{B} \text{ where } \vec{u} \text{ is fluid velocity along x-axis, the direction fluid flow.}$$

Thus,

$$\vec{j} \times \vec{B} = \sigma \vec{E} \times \vec{B}, = \sigma (\vec{u} \times \vec{B} \times \vec{B}) = \sigma \left((\vec{u} \cdot \vec{B}) \vec{B} - (\vec{B} \cdot \vec{B}) \vec{u} \right) \quad (1.22)$$

Using vector analysis laws (Murray, 1981) \vec{u} and \vec{B} in (1.22) are perpendicular vectors then $\vec{u} \cdot \vec{B} = 0$ hence the equation reduces to

$$\vec{j} \times \vec{B} = -\sigma B^2 \vec{u} \quad (1.23)$$

Substituting (1.23) in (1.21) it becomes

$$u \frac{\partial u}{\partial x} + v \frac{\partial u}{\partial y} = -\frac{1}{\rho} \frac{\partial p}{\partial x} + \frac{\mu}{\rho} \left(\frac{\partial^2 u}{\partial x^2} + \frac{\partial^2 u}{\partial y^2} \right) - \frac{\sigma B^2 u}{\rho} \quad (1.24)$$

Since there is no component of body force in y-direction $F_y = 0$ then equation (1.20) reduces to

$$u \frac{\partial v}{\partial x} + v \frac{\partial v}{\partial y} = -\frac{1}{\rho} \frac{\partial p}{\partial y} + \frac{\mu}{\rho} \left(\frac{\partial^2 v}{\partial x^2} + \frac{\partial^2 v}{\partial y^2} \right) \quad (1.25)$$

1.3.3 Equation of conservation of energy

This law can be derived by applying the first law of thermodynamics to the differential control volume in the flow field and it states that energy can neither be created nor destroyed, but can be transformed from one form to another. In thermodynamics, energy and work of a system are related in the first law which states that the rate of change of heat transferred into the system is equal to the total sum of the rate of internal energy and the work done on the system, that is

$$\frac{dQ}{dt} = \frac{dE}{dt} + \frac{dW}{dt} \quad (1.26)$$

where Q is amount of heat, E is internal energy and W is the work done by the system. The total rate of heat dQ within the system for an adiabatic (no heat is added nor removed from the system) process is the negative partial sum of heat along x and y coordinates within the system and is given by

$$\frac{dQ}{dt} = - \left(\frac{\partial Q_x}{\partial x} dx + \frac{\partial Q_y}{\partial y} dy \right) \quad (1.27)$$

The internal energy E in the fluid consists of the kinetic and potential energy and is described by

$$\frac{dE}{dt} = \rho \left[\frac{De}{Dt} + \frac{1}{2} \frac{D}{Dt} (u^2 + v^2) \right] dx dy \quad (1.28)$$

Where e is the internal energy per unit mass. The change in the internal energy of the system undergoing an adiabatic (no heat added or removed) change is equal to negative work done. This is so since internal energy is directly proportional to temperature of the system. The expression for work done on the system is

$$\frac{dW}{dt} = \frac{-dW_f}{dt} - \frac{dW_B}{dt} \quad (1.29)$$

where w_f is the work done by the frictional force within the system and w_B is the work done by the body (system). Substituting equations (1.27), (1.28) and (1.29) into (1.26) and simplifying it becomes

$$\rho \frac{De}{Dt} = K \left(\frac{\partial^2 T}{\partial x^2} + \frac{\partial^2 T}{\partial y^2} \right) + \mu \Phi \quad (1.30)$$

where the viscous- energy dissipation term Φ is express in Cartesian co-ordinates as

$$\Phi = 2 \left[\left(\frac{\partial u}{\partial x} \right)^2 + \left(\frac{\partial v}{\partial y} \right)^2 \right] + \left[\left(\frac{\partial u}{\partial y} + \frac{\partial v}{\partial x} \right)^2 \right] \quad (1.31)$$

1.3.4 Ohm's Law

Ohm's law characterizes the ability of material to transport electric charge under the influence of an applied electric field and states that the current through a conductor between two points is proportional to the voltage across the two points. Mathematically expressed as

$$V = IR \quad (1.32)$$

If we consider an electrically conducting fluid having a velocity \vec{u} and at right angles to a magnetic field \vec{B} and that a steady flow conditions are attained, then the interaction of these two fields induces an electric field \vec{E} at right angles to both \vec{u} and \vec{B} , thus

$$\vec{E} = \vec{u} \times \vec{B}. \quad (1.33)$$

By this law, the current density induced in the conducting fluid at stationary condition is given as

$$\vec{J} = \sigma \vec{E} \quad (1.33)$$

where, \vec{J} is the current density, σ is the conductivity parameter and \vec{E} is the electric field.

The generalized Ohm's law is given by

$$\vec{J} = \sigma(\vec{E} + \vec{u} \times \vec{B}) + \rho_c \vec{u} \quad (1.34)$$

Where $\rho_c \vec{u}$ represents the displacement current which is usually negligible at the fluid velocity \vec{u} , then the law reduces to Lorentz force which is the force associated with motion across a magnetic field and is given as

$$\vec{J} = \sigma(\vec{E} + \vec{u} \times \vec{B}) \quad (1.35)$$

1.3.5 Maxwell's equations

It's a set of four differential equations that describes the relationship between the electric and magnetic fields and their sources independent of the properties of matter.

Electric currents and charges in electric fields are proportional to the magnetic fields circulating about the areas they accumulate, that is

$$\vec{\nabla} \times \vec{B} = \mu \vec{j} + \mu \epsilon_0 \frac{\partial \vec{E}}{\partial t} \quad (\text{Ampere law}) \quad (1.36)$$

In the absence of magnetic monopoles, the magnetic field lines neither converge nor diverge thus

$$\vec{\nabla} \cdot \vec{B} = 0 \quad (\text{Gauss' law for magnetism}) \quad (1.37)$$

The voltage accumulated around a closed circuit is proportional to the time rate of change of the magnetic flux it encloses, thus

$$-\frac{\partial \vec{E}}{\partial t} = \vec{\nabla} \times \vec{E} \quad (\text{Faraday's law of induction}) \quad (1.38)$$

The electric field leaving a control volume is proportional to the charge inside, that is

$$\vec{\nabla} \cdot \epsilon_0 \vec{E} = \rho_e \quad (\text{Gauss' law for electricity}) \quad (1.39)$$

1.4 Statement of the problem

The steady hydromagnetic flow through a channel with two stationary parallel porous plates in the presence of magnetic field and an investigation of the effects of the porous plates when an electrically conducting fluid is placed in a magnetic field on the velocity and temperature distribution is considered. This investigation is used in finding an approximate solution for velocity profiles parallel and normal to the plates as well as the temperature distribution in the fluid.

1.5 Objectives of the study

1. To investigate the effect of porous plates of the hydromagnetic flow on fluid velocity parallel and normal to the plates.
2. To investigate the effect of Reynolds number and Hartmann number on the fluid flow.
3. To investigate the effect of Temperature distribution in the fluid flow

1.6 Significance of the study

The phenomenon of fluid flow between porous plates is of great theoretical as well as practical interest. Some of the practical interest includes problems dealing with gaseous diffusion, transpiration-cooling, lubrication of porous bearings and walled flow reactors. It's also encountered in a wide range of engineering and industrial applications such as in recovery or extraction of crude oil, geothermal systems, and thermal insulation and in boundary layer control in the field of aerodynamics. This study is important in the study of constant leakage of oil from the piston cylinder hydraulic system where we assume the piston is stationary and the gap width is small, hence the flow between fixed parallel plates. Therefore there is need to study hydromagnetic flow of steady incompressible fluid between parallel porous plates.

CHAPTER TWO

LITERATURE REVIEW

2.1 Introduction

The steady hydromagnetic fluid flow of a Newtonian electrically conducting viscous incompressible and radiating fluid between two parallel porous plates has been studied by many engineers and scientists. The study of magnetohydrodynamic (MHD) is largely perceived to have been studied by Michael Faraday (26th July 2016, Tuesday at 1900 hrs) when he tried to examine the ebbing salty water flowing past London's Waterloo bridge. He later did another experiment with mercury as conducting fluid where he studied the behavior of current in a circuit placed in time varying magnetic fields and observed that a voltage was induced in the direction perpendicular to both the direction of the flow and magnetic field. He further showed that when an electric field is applied to a conducting fluid in the direction which is perpendicular to magnetic field, a force is exerted on the fluid in the direction perpendicular to both electric field and magnetic field. Since then a lot has been done on MHD and its related fields.

2.2 Literature review

Govinda and Jain (1966) studied hydromagnetic laminar flow through conducting parallel porous plates where they took the porosity of the walls into account. In their study they considered a rectangular channel when the total current was zero and when it was not zero. They found that the general solution had two unknown constants. They showed that when these constants are chosen the general solution can be made to fit the solution of

two dimensional channels whose geometry approaches the limit to that of one dimensional channel. Rao and Vdyanidhl (1969) studied two dimensional unsteady flow of a conducting viscous incompressible fluid between parallel porous plates where one was fixed while the other one was uniformly accelerated in a transverse magnetic field. They found that for a given Hartmann number, a suction parameter increases velocity at any point of the fluid while the skin friction at the stationary plate increases and that of the accelerated plate decreases. Greif *et al* (1971) obtained an exact solution for the problem of laminar convective flow in a vertical heated channel within the optically thin limit. Kearsley (1994) studied the problem of steady state couette flow with viscous heating and found an exact solution for non linear problem with thermal mechanical coupling. The steady flow of the fluid with viscosity exponentially depended on temperature which was shared between an adiabatic fixed inner cylinder and thermos rotating outer cylinder. He found that there was maximum torque above which no steady flow was possible and below which flows were possible, a high shear and a low shear steady flow for each value was realized.

Raptis *et al* (1982) analyzed the problem of hydromagnetic free convection flow through a porous medium between two parallel plates. In their study, the effects of buoyancy, boundary and inertia of porous media were discussed as well as Hartmann effects on MHD and heat generation or absorption of fluid were also discussed and resulting ordinary differential equations were solved.

Daskalaski (1990) studied on the couette flow through a porous medium of a high Prandtl number fluid with temperature dependent viscosity. He concluded that, in the steady state the medium permeability for both velocity and temperature profiles are positively skew

and its skewness increases with permeability. Albarbi (2010) studied convective heat and mass transfer characteristics of an incompressible MHD visco-elastic fluid flow through a porous medium over a stretching sheet with chemical reaction and thermal stratification. It was found that both temperature and concentration increase with increasing visco-elastic parameter, porosity parameter and magnetic parameter. In addition, the velocity profile and temperature profile increase with the increase of heat absorption parameter and decrease with increasing chemical reaction.

Bhargava and Takhar (2001) studied the numerical solution of free convection MHD micropolar fluid between two parallel porous vertical plates. The basics of electromagnetic induction were reviewed and the magnetic Reynolds number due to Ohmic resistance was defined. For the case of a perfectly conducting fluid, Alfven's frozen flux theorem was derived. They studied the presence of temperature dependent heat sources and the effect of friction heating in the presence of magnetic field. The profiles for velocity, microrotation and temperature were presented for a wide range of Hartmann numbers and micropolar parameter. The skin friction, couple stress and Nusselt numbers at the plates were shown in the tables. Aristov and Gitman (2002) studied the motion of a viscous incompressible liquid between two parallel disks moving towards each other. They analyzed the possible descriptions of motion based on the exact solution of Navier-Stokes equation and the stability of the motion for different initial perturbations. Hazeem (2006) investigated the effect of variable viscosity on the transient Couette flow of dusty fluid with heat transfer between parallel plates. He showed some important effects for the viscosity and uniform magnetic field on the transient flow and heat transfer of both the fluid and dusty particles. Attia (1997) analyzed the transient

MHD flow and heat transfer between two parallel plates with temperature dependent viscosity while Sharma *et al* (2005) explained the steady laminar flow and heat of a non-Newtonian fluid through a straight horizontal porous channel in the presence of heat source.

Okelo (2007) investigated unsteady free convection incompressible fluid past a semi-infinite vertical porous plate in the presence of a strong magnetic field inclined at an angle to the plane with hall and ion slip current effects. He found that an increase in mass diffusion parameter caused an increase in the concentration profile, while an increase in Eckert number caused an increase in temperature profile. He further observed that an increase in the angle of inclination lead to an increase in primary velocity profiles but a decrease in secondary profiles. Guria (2008) studied hydromagnetic flow between two porous disks rotating about non coincident axes. He found that the temperature increased with increase in either Hartmann number or thermal conductivity and that the rate of heat increased with increase in temperature. Das *et al* (2008) analyzed a three dimensional couette flow of a viscous incompressible electrically conducting fluid between two infinite horizontal parallel porous flat plates in the presence of a transverse magnetic field. The governing equations were solved by using the series expansion method and the expressions for the velocity field, temperature field, skin friction and heat flux in terms of Nusselt number was obtained. They found that magnetic parameter retards the main fluid velocity and accelerates radial velocity of the flow field. Israel –Cookey and Nwaigwe (2010) considered unsteady MHD flow of a rotating fluid over a vertical moving heated porous plate with time-dependent suction. In their study closed form analytical solutions were constructed for the problem, the results were discussed quantitatively with the aid of

dimensionless parameters. Screenivasulup *et al* (2013) investigated the effects of radiation on MHD flow. They found that magnetic field reduced the fluid velocity but increase the temperature while Ramesh and Murulidhara (2013) provided a numerical solution of the MHD Reynolds equations for squeeze-film lubrication between porous and rough rectangular plates. Baoku *et al* (2010) examined the problem of hydromagnetic Couette flow of a high viscous fluid through a channel in the presence of an applied uniform transverse magnetic field and thermal radiation. They found that an increase in thermal radiation results in a decrease in the temperature profiles of the hydromagnetic Couette fluid and the increase in magnetic field lead to an increase in the velocity profiles.

Kumar *et al* (2010) considered the problem of unsteady MHD periodic flow of viscous fluid through a planar channel in a porous medium using perturbation techniques. Singh (2014) studied a steady laminar flow of viscous incompressible fluid between two parallel infinite plates under applied pressure gradient when upper plate is moving with constant velocity and lower plate is held stationary under the influence of inclined magnetic field. The Laplace transform method was used to solve the governing equations. The expression for fluid velocity at different strengths of magnetic field and at different inclination was shown graphically. The results showed that increase in inclination of magnetic field produced a decrease in velocity profile. Manyonge *et al* (2012) examined the motion of a two dimensional steady flow of a viscous, electrically conducting incompressible fluid flowing between two infinite parallel plates where the lower plate was porous and upper not. The parallel plates were under the influence of transverse magnetic field and constant pressure gradient. The resulting differential equations were

solved using analytical method and solutions expressed in terms of Hartmann number and the effects of magnetic inclinations to velocity were discussed graphically.

In this study, it considers a hydromagnetic flow of a steady two dimensional laminar flow of an incompressible viscous fluid between parallel stationary porous plates in the presence of transverse magnetic field by finding the approximate solution for velocity profile parallel and normal to the wall plates and the temperature distribution in the flow which previous studies had not considered.

CHAPTER THREE

METHODOLOGY

3.1 Introduction

In this chapter, the discussion of formulation of the problem, assumptions and approximations, boundary conditions, non dimensionalization and the solution of the third order partial differential equation of an incompressible flow by the method of regular perturbation and the power series expansion are considered.

3.2 Formulation of the problem

The steady laminar flow of an incompressible viscous conducting fluid with a small electrical conductivity defined by the scalar quantity σ between the two parallel stationary non conducting porous plates in the presence of a uniform transverse magnetic field \vec{B} and with the main fluid velocity U along x -axis, the fluid flow direction is considered. Assuming that the conducting fluid is isotropic, the interaction of magnetic field and the induced current density produces an electromotive force, \mathbf{F} and both the two porous plates are taken to have equal porosity. A Cartesian coordinate system (x, y, z) where x, y and z are the coordinate axes is chosen.

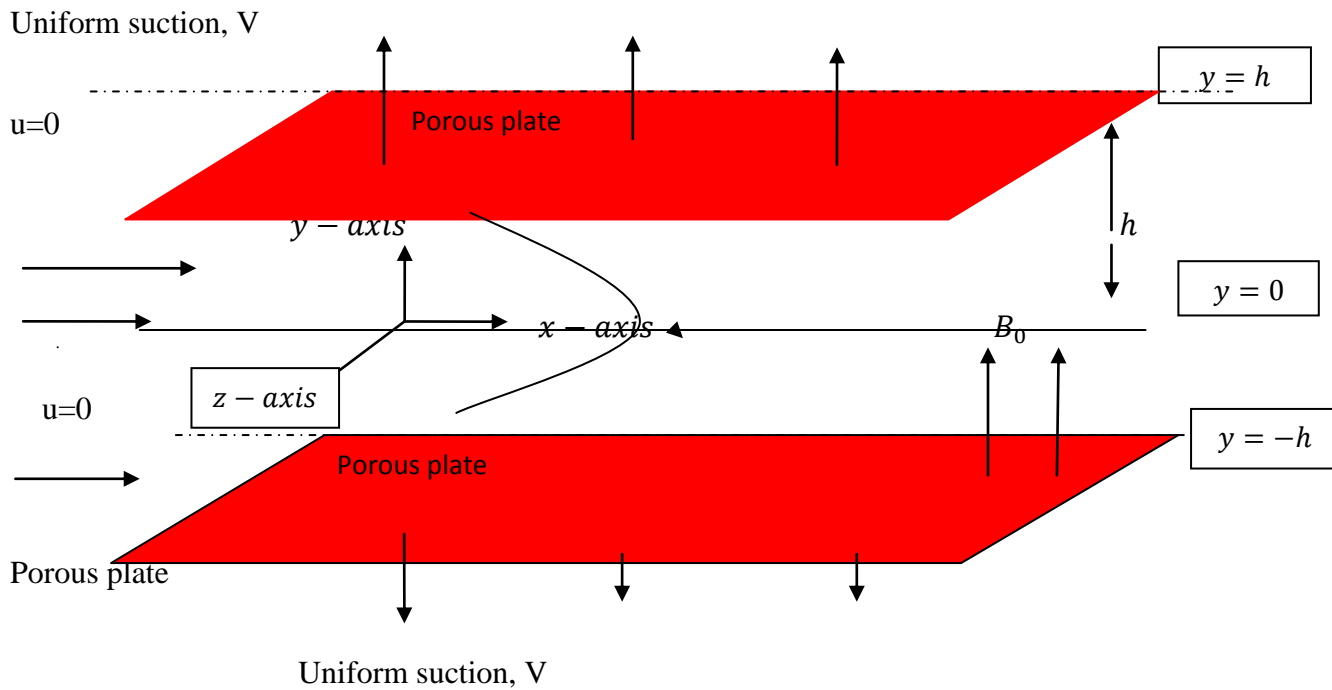


Figure 3.1 The physical configuration of the problem

The x and y are parallel and perpendicular to the channel walls respectively and the origin is taken at the centre of the channel. The length of the plates is assumed to be L and $2h$ is the distance between the two parallel plates. The plates are of infinite length in z -direction; therefore all the physical quantities involved are independent of z for this fully developed laminar flow thus the problem is a two-dimensional. The upper and the lower plates are subjected to a constant suction, $V(> 0)$ due to electromotive force occurring simultaneously with the induced current. Denoting u, v and w to be the components of velocity in the directions of x, y and z increasing respectively as shown in the figure 3.1. The value of $w = 0$ since the velocity along this axis is independent of z .

3.2.1 Assumptions and approximations

The following assumptions and approximations are made;

- There is uniform withdrawal of fluid at the porous plates
- The porous plates are non-conducting
- No chemical reaction is taking place in the fluid
- No external electric field and induced magnetic field in the flow
- The fluid is Newtonian such that fluid viscosity is assumed constant
- The fluid is steady, incompressible and laminar
- The magnetic Reynolds number is very small
- There is no joules heating effect in the flow
- The flow is limited to slow speed ($v, u \ll c$)

From the above assumptions and approximations the equations (1.11), (1.24), (1.25) and (1.30) then becomes the governing equations for the steady hydromagnetic flow.

From the diagram of Figure 3.1 above the velocity at any cross-section of the channel varies from the walls of the porous plates to a maximum at the centre when there is no magnetic field indicating that there is a well defined free stream otherwise affected by the porous nature of the plates.

3.2.2 Conditions at the porous plate

The conditions for the hydromagnetic flow through a channel with parallel porous plates where the fluid is withdrawn from both walls of the channel at the same rate are complicated by the type of porosity of the plates and the no-slip condition is relaxed on

the velocity component normal to the walls of the plates. Therefore, the general conditions are as follows:

$$V_{\text{tangential}}: u(x, h) = 0, u(x, -h) = 0 \text{ (No-slip condition)} \quad (3.1)$$

$$V_{\text{normal}}: v(x, h) = V, \text{ and } v(x, -h) = -V \text{ (Flow through wall)} \quad (3.2)$$

where V is the suction velocity at the plates of the channel and h is the channel width from the axis of the channel to the plates.

The temperature conditions are also complicated by a porous wall in that the suction at the plate walls where the fluid leaves the main flow and passes into the wall is sufficiently accurate to assume that: $T_{\text{fluid}} = T_{\text{wall}}$

$$T = \begin{cases} T_w & y = \pm h \\ T_0 & y = 0 \end{cases} \quad (3.3)$$

3.2.3 Non-dimensionalization

To dimensionless the equations (1.1), (1.25) and (1.6)

Let

$$\eta = \frac{y}{h} \Rightarrow \partial\eta = \frac{\partial y}{h} \quad (3.4)$$

Substituting the non-dimensional equation (3.4) into equations (1.1), (1.25) and (1.6) it becomes

$$\frac{\partial u}{\partial x} + \frac{\partial v}{h \partial \eta} = 0 \quad (3.5)$$

$$u \frac{\partial u}{\partial x} + \frac{v \partial v}{h \partial \eta} = \frac{-1}{\rho} \frac{\partial p}{\partial x} + v \left(\frac{\partial^2 u}{\partial x^2} + \frac{1}{h^2} \frac{\partial^2 u}{\partial \eta^2} \right) - \frac{\sigma B^2 u}{\rho} \quad (3.6)$$

$$u \frac{\partial v}{\partial x} + \frac{v}{h} \frac{\partial v}{\partial \eta} = \frac{1}{\rho h} \frac{\partial p}{\partial \eta} + v \left(\frac{\partial^2 v}{\partial x^2} + \frac{1}{h^2} \frac{\partial^2 u}{\partial \eta^2} \right) \quad (3.7)$$

Equations (3.5), (3.6), and (3.7) give the dimensionless form of the governing equations.

The boundary conditions (3.1) and (3.2) then reduces to

$$u(x, 1) = 0, \quad u(x, -1) = 0 \text{ and } v(x, 1) = V, v(x, -1) = -V \quad (3.8)$$

In describing the fluid flow, the stream function plays a great role since it is a scalar function of space and time. Its partial derivative with respect to any direction gives the velocity component at right angles to the direction. For steady flow, it's defined as $\psi = f(x)$ such that

$$u(x, \eta) = \partial\psi/\partial y \text{ and } v(x, \eta) = -\partial\psi/\partial x \quad (3.9)$$

The dimensionless form of (3.9) becomes

$$u = \frac{1}{h} \frac{\partial\psi}{\partial \eta}, v = -\frac{\partial\psi}{\partial x} \quad (3.10)$$

The equation of continuity can be satisfied by a stream function of the form

$$\psi(x, y) = [hU(0) - Vx]f(\eta) \quad (3.11)$$

where $U(0)$ is the average entrance velocity at $x = 0$. Differentiating equation (3.11) with respect to η and x and substituting into equation (3.10) the velocity components becomes

$$u = \frac{\partial\psi}{\partial y} = \frac{1}{h} [hU(0) - Vx]f_\eta(\eta) \quad (3.12)$$

and

$$v = -\frac{\partial \psi}{\partial x} = Vf(\eta) \quad (3.13)$$

where $f_\eta(\eta)$ is the partial differentiation with respect to the dimensionless variable η .

Since we are considering a situation when the fluid is being withdrawn at constant rate from both the walls, then V is independent of x and using (3.12) and (3.13) in (3.6) and (3.7) the equation of momentum reduces to

$$-\frac{1}{\rho} \frac{\partial p}{\partial x} = \left[\left(U(0) - \frac{Vx}{h} \right) \left(\frac{V}{h} (ff_\eta - f_\eta^2) - \frac{v}{h^2} f_{\eta\eta\eta} + \frac{\sigma B^2}{\rho} f_\eta \right) \right] \quad (3.14)$$

or

$$-\frac{1}{h\rho} \frac{\partial p}{\partial \eta} = \frac{V^2}{h} ff_\eta - \frac{vV}{h^2} f_{\eta\eta} \quad (3.15)$$

Differentiating (3.15) with respect to η becomes

$$\frac{\partial^2 p}{\partial x \partial \eta} = \left(U(0) - \frac{Vx}{h} \right) \frac{\partial}{\partial \eta} \left[\frac{V}{h} (ff_{\eta\eta} - f_\eta^2) - \frac{v}{h^2} f_{\eta\eta\eta} + \frac{\sigma B^2}{\rho} f_\eta \right] \quad (3.16)$$

Also differentiating (3.15) with respect to x and simplifying becomes

$$\frac{\partial^2 p}{\partial x \partial \eta} = 0 \quad (3.17)$$

Substituting equation (3.17) into equation (3.16) and simplifying becomes

$$\frac{\partial}{\partial \eta} \left[\frac{V}{h} (ff_{\eta\eta} - f_\eta^2) - \frac{v}{h^2} f_{\eta\eta\eta} + \frac{\sigma B^2}{\rho} f_\eta \right] = 0 \quad (3.18)$$

Integrating (3.18) with respect to η and substituting the dimensionless parameters (Reynolds number, R and Hartmann number, M) become

$$f_{\eta\eta\eta} + R(f_{\eta}^2 - f f_{\eta\eta}) - \varepsilon R f_{\eta} = K \quad (3.19)$$

Where $\varepsilon = \frac{H_0^2 \mu_e^2 \sigma h}{\rho \nu}$, $R = \frac{\rho u l}{\mu} = \frac{u l}{\nu}$ and K is an arbitrary constant to be determined.

The solution of the equations of motion and continuity is given by a non linear third order partial differential equation (3.19) which is to be solved by perturbation method when R and ε are small subject to the boundary conditions on $f(\eta)$ which are:

$$f(1) = 1, f(-1) = -1, f_{\eta}(1) = 0, \text{ and } f_{\eta}(-1) = 0 \quad (3.20)$$

And

$$f_0(-1) = -1, f_{0\eta}(0) = 0, f_0(1) = 1, f_{0\eta}(1) = 0 \quad (3.21)$$

The energy equation is
$$u \frac{\partial T}{\partial x} + v \frac{\partial T}{\partial y} = \alpha \frac{\partial^2 T}{\partial y^2} + \frac{\nu}{c_p} \left(\frac{\partial u}{\partial y} \right)^2 \quad (3.22)$$

Using the conditions

$$T = \begin{cases} T_{\infty}, y = \infty \\ T_0, y = 0 \end{cases} \quad (3.23)$$

and assuming $v = 0, u = \left(\frac{y}{L}\right) U$ and $T = T(y)$ (3.24)

Equation (3.22) becomes

$$0 = \alpha \frac{\partial^2 T}{\partial y^2} + \frac{\nu}{c_p} \left(\frac{\partial u}{\partial y} \right)^2 \text{ or } k \frac{\partial^2 T}{\partial y^2} + \mu \left(\frac{\partial u}{\partial y} \right)^2 = 0 \Rightarrow \frac{\partial^2 T}{\partial y^2} = -\frac{\mu}{k} \left(\frac{U}{L} \right)^2 \quad (3.25)$$

Integrating (3.22) twice with respect to y we get

$$T(y) = \frac{\mu}{2k} \left(\frac{U}{L}\right)^2 y^2 + c_1 y + c_2 \quad (3.26)$$

The boundary conditions for temperature when $y = 0$ is $T = T_0$ and when $y = h$ is $T = T_h$ applying these boundary conditions in (3.26) gives the temperature distribution as

$$T(y) = T_0 + \frac{\mu U^2}{2k} \left[\frac{y}{L} - \left(\frac{y}{L}\right)^2 \right] + (T_h - T_0) \frac{y}{L} \quad (3.28)$$

which in the dimensionless form is

$$\frac{T(y)-T_0}{T_w-T_0} = \frac{y}{L} \left[1 + \frac{\mu U^2}{2k(T_L-T_0)} \left(1 - \frac{y}{L} \right) \right] \quad (3.29)$$

Or

$$\theta(\eta) = \eta \left[1 + \frac{1}{2} P_r \right] E (1 - \eta) \quad (3.30)$$

where various non-dimensional qualities are defined as

$$\theta(\eta) = \frac{T(y)-T_0}{T_w-T_0}, \text{ non-dimensional temperature} \quad (3.31)$$

$$\eta = \frac{y}{L}, \text{ dimensionless length,} \quad (3.32)$$

$$P_r = \frac{\mu c_p}{k}, \text{ Prandtl number} \quad (3.33)$$

$$E = \frac{U^2}{c_p(T_h-T_0)}, \text{ Eckert number} \quad (3.34)$$

3.3 Perturbation Theory

The theory deals with mathematical methods for finding an approximate solution to a problem by starting from an exact solution of a related simpler problem and breaking it into a solvable part. It is applicable if the problem at hand cannot be solved exactly, but can be formulated by adding a small term to the mathematical description of the exactly solvable problem. This leads to an expression for the desired solution in terms of a power series in the small parameter. The solution of nonlinear partial differential equations in fluid mechanics has been of importance since the basic nonlinearity exact solutions are rare thus we approximate. Approximations are used when one or more of the parameters in the problem are small. The dimensionless parameters such as Reynolds, Hartmann, Prandtl and Eckert numbers are amongst many in fluid dynamics used as the perturbation quantity. This quantity when it tends to zero makes the approximation becomes accurate. In practice, we usually calculate the exact first approximation known as rational approximation while on the other hand, useful approximations do not become exact in any known limit thus become irrational (represents dead end). In this thesis, we shall deal with rational approximation which concerns with asymptotic expansions for small values of parameter of the solutions of the equation of fluid motion. In parameter perturbations the basic solution is often a uniform parallel stream flow which is referred to as ‘zeroth approximation’ from the first approximation or first-order solution.

A perturbation solution which leads to satisfactory results and the series cannot converge for the small parameter everywhere in the flow field is called regular perturbation while singular perturbation is one in which the straightforward perturbation solution is not uniformly valid throughout the flow field and become worse rather than better. For this

thesis, the regular perturbation method is used because the reasonably small parameter is everywhere uniform in the flow field and appears to be true. Due to the exact solutions being rare for non linear problems, a single exact solution is perturbed in a number of ways to explore different effects and the following regular perturbation procedures are adopted which consists of:

- a) Substituting the power series $y(\eta, R) \approx \sum_{n=0}^{\infty} R^n f_n(\eta)$ into the partial differential equation and the boundary conditions
- b) Expanding the quantities in a power series in R
- c) Collecting terms with same powers of R and equating them to zero
- d) Solving the hierarchy of boundary value problems sequentially.

Therefore investigating the solution of equation (3.19) subject to the boundary conditions (3.20) and (3.21) by the above procedure and considering the case when R and ε are small we approximate the analytic results that will be obtained by using the method of regular perturbation approach and Taylor's expansion. The non-linear nature of equation (3.19) preclude its exact solution hence we seek the solution in the form of power series in R , that is

$$f = \sum_{n=0}^{\infty} R^n f_n(\eta) = f_0(\eta) + R^1 f_1(\eta) + R^2 f_2(\eta) \quad (3.33)$$

Or

$$k = \sum_{n=0}^{\infty} k_n R^n = k_0 + R^1 k_1 + R^2 k_2 + \dots \quad (3.34)$$

Differentiating successively the partial differential equation (3.33) with respect to η we get

$$\left. \begin{aligned} f_\eta &= f_{0\eta} + Rf_{1\eta} + R^2f_{2\eta} + \dots \\ f_{\eta\eta} &= f_{0\eta\eta} + Rf_{1\eta\eta} + R^2f_{2\eta\eta} + \dots \\ f_{\eta\eta\eta} &= f_{0\eta\eta\eta} + Rf_{1\eta\eta\eta} + R^2f_{2\eta\eta\eta} + \dots \end{aligned} \right\} \quad (3.35)$$

Substituting equation (3.34) and (3.35) into (3.19) becomes

$$\begin{aligned} & \left(f_{0\eta\eta\eta} + Rf_{1\eta\eta\eta} + R^2f_{2\eta\eta\eta} + \dots \right) + R \left[\left(f_{0\eta} + Rf_{1\eta} + R^2f_{2\eta} + \dots \right)^2 - \right. \\ & \quad \left. \left\{ \left(f_0 + Rf_1 + R^2f_2 + \dots \right) \left(f_{0\eta\eta} + Rf_{1\eta\eta} + R^2f_{2\eta\eta} + \dots \right) \right\} \right. \\ & \quad \left. - \varepsilon \left(f_{0\eta} + Rf_{1\eta} + R^2f_{2\eta} + \dots \right) \right] \\ & = k_0 + Rk_1 + R^2k_2 \end{aligned} \quad (3.36)$$

Expanding the expression (3.36) gives

$$\begin{aligned} & f_{0\eta\eta\eta} + R \left[f_{0\eta\eta\eta} + f_{0\eta}^2 - f_0f_{1\eta\eta} - \varepsilon f_{0\eta} + \dots \right] + R^2 \left[f_{2\eta\eta\eta} + 2f_{0\eta}f_{1\eta} - f_0f_{1\eta\eta} - \right. \\ & \left. f_{0\eta\eta}f_1 - \varepsilon f_{1\eta} + \dots \right] + R^3 \left[f_{3\eta\eta\eta} + f_{0\eta}f_{2\eta} + f_{1\eta}^2 + \dots \right] = k_0 + Rk_1 + R^2k_2 + \dots \end{aligned} \quad (3.37)$$

Equating the coefficients of R becomes

$$f_{0\eta\eta\eta} = k_0 \quad (3.38)$$

$$f_{1\eta\eta\eta} + f_{0\eta}^2 - f_0f_{1\eta\eta} - \varepsilon f_{0\eta} = k_1 \quad (3.39)$$

$$f_{2\eta\eta\eta} + 2f_{0\eta}f_{1\eta} - f_0f_{1\eta\eta} - f_{0\eta\eta}f_1 - \varepsilon f_{1\eta} = k_2 \quad (3.40)$$

.

.

.

and so on.

Integrating equation (3.39) twice becomes

$$\left. \begin{aligned} f_{0\eta\eta} &= k_0\eta + A \\ f_{0\eta}(\eta) &= \frac{k_0\eta^2}{2} + A\eta + B \\ f_0(\eta) &= \frac{k_0}{6}\eta^3 + \frac{A}{2}\eta^2 + B\eta + C \end{aligned} \right\} \quad (3.41)$$

Solving simultaneously the derived equations (3.41) subject to conditions (3.20) and (3.21) gives

$$A = 0, B = \frac{3}{2}, C = 0, \text{ and } k_1 = -3 \quad (3.42)$$

Thus the solution to (3.38) becomes

$$f_0(\eta) = \frac{\eta}{2}(3 - \eta^2) \quad (3.45)$$

Solving equation (3.37) using the derivatives of (3.43) gives

$$f_{1\eta\eta\eta} = k_1 + \frac{3}{2}\varepsilon - \frac{15}{4}\eta^4 - \left(\frac{3\varepsilon-9}{2}\right)\eta^2 - \frac{9}{4} \quad (3.44)$$

Integrating (3.41) thrice becomes

$$f_{1\eta\eta} = \left(k_1 + \frac{3\varepsilon}{2} - \frac{9}{4}\right)\eta - \frac{3}{20}\eta^5 - \left(\frac{\varepsilon}{2}\right)\eta^3 + A \quad (3.45)$$

$$f_{1\eta} = \left(\frac{k_1}{2} + \frac{3\varepsilon}{4} - \frac{9}{8}\right)\eta^2 - \frac{\eta^6}{40} - \left(\frac{\varepsilon}{8}\right)\eta^4 + A\eta + B \quad (3.46)$$

$$f_1 = \left(\frac{k_1}{6} + \frac{\varepsilon}{4} - \frac{3}{8}\right)\eta^3 - \frac{\eta^7}{280} - \left(\frac{\varepsilon}{40}\right)\eta^5 + \frac{A\eta^2}{2} + B\eta + C \quad (3.47)$$

Solving equations (3.45-3.47) subject to the boundary conditions (3.20) and (3.21) and simplifying equation (3.47) becomes

$$f_1(\eta) = 0.010714285\eta^3 - 0.003571429\eta^7 - 0.025\varepsilon\eta^5 - 0.025\varepsilon\eta - 0.007142857\eta + 0.05\varepsilon\eta^3 \quad (3.48)$$

The first order perturbation solutions for $f(\eta)$ is given by

$$f^{(1)}(\eta) = f_0(\eta) + Rf_1(\eta) \quad (3.49)$$

Substituting (3.43) and (3.48) into (3.49) the first order perturbation solution becomes

$$f^{(1)}(\eta) = \frac{\eta}{2}(3 - \eta^2) + 0.010714285R\eta^3 - 0.003571429R\eta^7 - 0.025M^2\eta^5 - 0.025M^2\eta - 0.007142857R\eta + 0.05M^2\eta^3 \quad (3.50)$$

And for k is given by

$$k^{(1)} = k_0 + Rk_1, \text{ that is } k^{(1)} = -3 - 1.2M^2 + 2.314285714R \quad (3.51)$$

where $M^2 = \varepsilon R$ in the above equations (3.50) and (3.51).

Solving equation (3.40) using (3.43), (3.48), their derivatives and anti-derivatives as in the procedure of solution of (3.39) subject to the boundary conditions (3.20) and (3.21) gives

$$\begin{aligned}
f_2 = & \\
& (0.0013\varepsilon^2 - 0.00209\varepsilon - 0.00054)\eta + \\
& (0.00671 + 0.0027695\varepsilon - 0.003211667\varepsilon^2)\eta^3 + (0.214285714\varepsilon + 0.0025\varepsilon^2)\eta^5 + \\
& (0.000153061 - 0.001071429\varepsilon - 0.000595238\varepsilon^2)\eta^7 - (0.000297619 + \\
& 0.000148810\varepsilon)\eta^9 + 0.000010823\eta^{11} \tag{3.52}
\end{aligned}$$

and

$$k_2 = 0.0057\varepsilon^2 - 0.0512\varepsilon - 0.0174 \tag{3.53}$$

Thus the second order perturbation solutions for $f(\eta)$ is given by

$$f^{(2)}(\eta) = f_0(\eta) + Rf_1(\eta) + R^2f_2(\eta) \tag{3.54}$$

Substituting (3.43), (3.48) and (3.52) in (3.54) and then simplifying the expressions, the second order perturbation becomes

$$\begin{aligned}
f^{(2)}(\eta) = & \frac{\eta}{2}(3 - \eta^2) + 0.010714285\eta^3 - 0.003571429\eta^7 - 0.025\varepsilon\eta^5 - 0.025\varepsilon\eta - \\
& 0.007142857\eta + 0.05\varepsilon\eta^3 + (0.0013\varepsilon^2 - 0.00209\varepsilon - 0.00054)\eta + (0.00671 + \\
& 0.0027695\varepsilon - 0.003211667\varepsilon^2)\eta^3 + (0.214285714\varepsilon + 0.0025\varepsilon^2)\eta^5 + \\
& (0.000153061 - 0.001071429\varepsilon - 0.000595238\varepsilon^2)\eta^7 - (0.000297619 + \\
& 0.000148810\varepsilon)\eta^9 + 0.000010823\eta^{11} \tag{3.55}
\end{aligned}$$

$$\text{And the second perturbation for } k \text{ is } k^{(2)} = k^{(1)} + k_2R^2 \tag{3.56}$$

Substituting (3.51) and (3.53) in (3.56) gives

$$k^{(2)} = -3 - 1.2M^2 + 2.314285714R + 0.0057M^4 - 0.0512M^2R - 0.0174R^2 \quad (3.57)$$

$$\text{where } \varepsilon R = M^2, \varepsilon R^2 = \varepsilon R, R = M^2R, \varepsilon^2 R^2 = M^4$$

The first order expressions for the velocity components are given by (3.12) and (3.13). The derivative of (3.50) is

$$f_\eta(\eta) = \frac{3}{2}(1 - \eta^2) + 0.032142855R\eta^2 - 0.021428574R\eta^6 - 0.1M^2\eta^4 - 0.025M^2 - 0.007142857R - 0.15M^2\eta^2 \quad (3.58)$$

Substituting (3.60) and (3.50) in (3.12) and (3.13) respectively gives

$$u(x, \eta) = \left(U(0) - \frac{Vx}{h} \right) \left[\frac{3}{2}(1 - \eta^2) + 0.032142855R\eta^2 - 0.021428574R\eta^6 - 0.1M^2\eta^4 - 0.025M^2 - 0.007142857R - 0.15M^2\eta^2 \right] \quad (3.59)$$

And

$$v(\eta) = Vf(\eta) = V \left[\frac{\eta}{2}(3 - \eta^2) + 0.010714285R\eta^3 - 0.003571429R\eta^7 - 0.025M^2\eta^5 - 0.025M^2\eta - 0.007142857R\eta + 0.05M^2\eta^3 \right] \quad (3.60)$$

From (3.59), $U(0)$ is the average entrance velocity and V is the suction velocity. Since the fluid is being withdrawn at the same rate from both porous walls, therefore the suction velocity, V is independent of x hence Vx can be fixed. This means that the flow along the vertical and the horizontal axes are constant and only depends on the Reynolds's number R and Hartmann's number M^2 .

Therefore the radial velocity v_r (parallel to y-axis) becomes

$$f(\eta) = v_r = \frac{\eta}{2}(3 - \eta^2) + 0.010714285R\eta^3 - 0.003571429R\eta^7 - 0.025M^2\eta^5 - 0.025M^2\eta - 0.007142857R\eta + 0.05M^2\eta^3 \quad (3.61)$$

And the axial velocity v_a (parallel to x-axis) becomes

$$f_\eta(\eta) = v_a = \frac{3}{2}(1 - \eta^2) + 0.032142855R\eta^2 - 0.021428574R\eta^6 - 0.1M^2\eta^4 - 0.025M^2 - 0.007142857R - 0.15M^2\eta^2 \quad (3.62)$$

To investigate the effects of porous plates on velocity profiles in the hydromagnetic flow, the values of radial velocity, v_r and axial velocity, v_a are plotted against non dimensional length, η as the values of the suction Reynolds number, R and the Hartmann number, M are varied as discussed in the next chapter.

CHAPTER FOUR

RESULTS AND DISCUSSION

4.1 Introduction

In this chapter, the results of the radial velocity, axial velocity and temperature profiles of the hydromagnetic flow are presented and the results were generated by the MATLAB software.

4.2 Results

4.2.1 Radial velocity, v_r

Considering equation (3.61), the values of radial velocity, v_r are plotted against the non dimensional length, η as the values of suction Reynolds number, R and Hartmann number, M are varied. Figure 4.1 shows the variation of radial velocity, v_r with the non dimensional variable, η and its corresponding table is presented in table A1 in the appendix A.

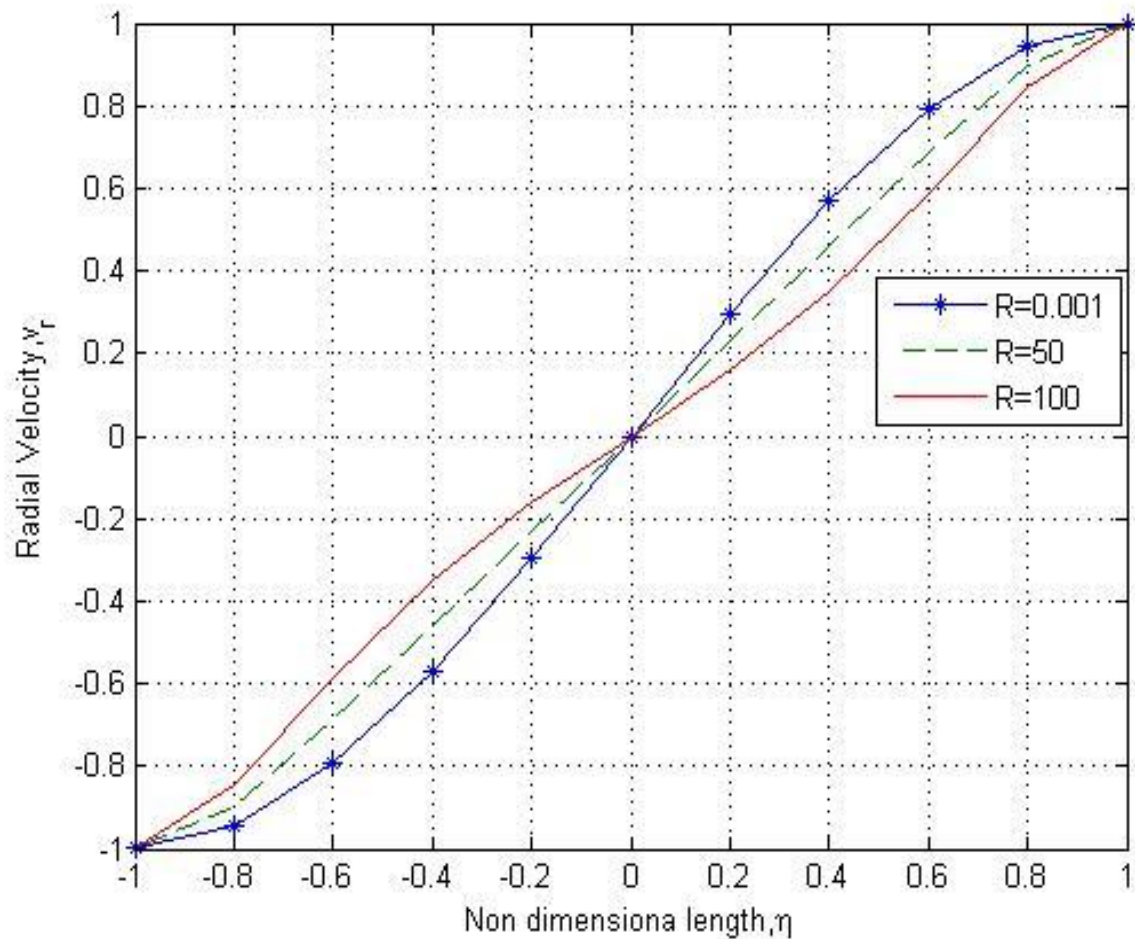


Figure 4.1: Radial velocity profiles as a function of η for constant $M=0$ and varying R .

In the figure 4.1, it is observed that the radial velocity decreases as Reynolds number increases when Hartman number is zero, but increases from the central region of the flow towards the plates as the non dimensional length increases. It is observed that when the fluid is non MHD ($M=0$) there is no magnetic field existing in the flow thus reduces the radial velocity. When the viscous forces in the flow becomes very small the inertia forces dominates thus increases the radial velocity towards the porous plates.

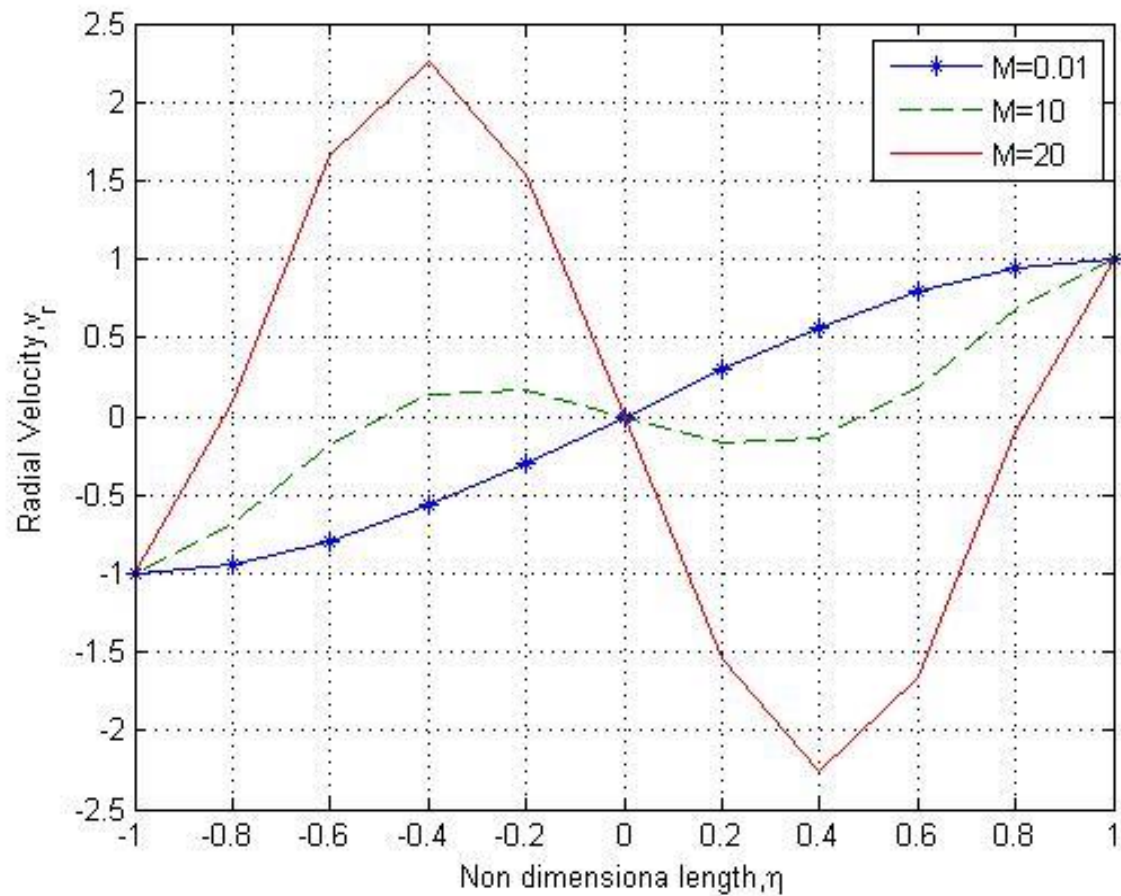


Figure 4.2: Radial velocity profiles as a function of η for constant $R=0.001$ and varying M .

In Figure 4.2, it's observed that for different values of increasing M in the region

$-1 \leq \eta \leq 0$, radial velocity, v_r Increases with small values of R because inertia forces are negligible while in the region

$0 \leq \eta \leq 1$, radial velocity, v_r decreases with the increase of M significantly. When M and R are significantly small the radial velocity is less sinusoidal about the centre of the flow and increases as the non dimensional numbers increases

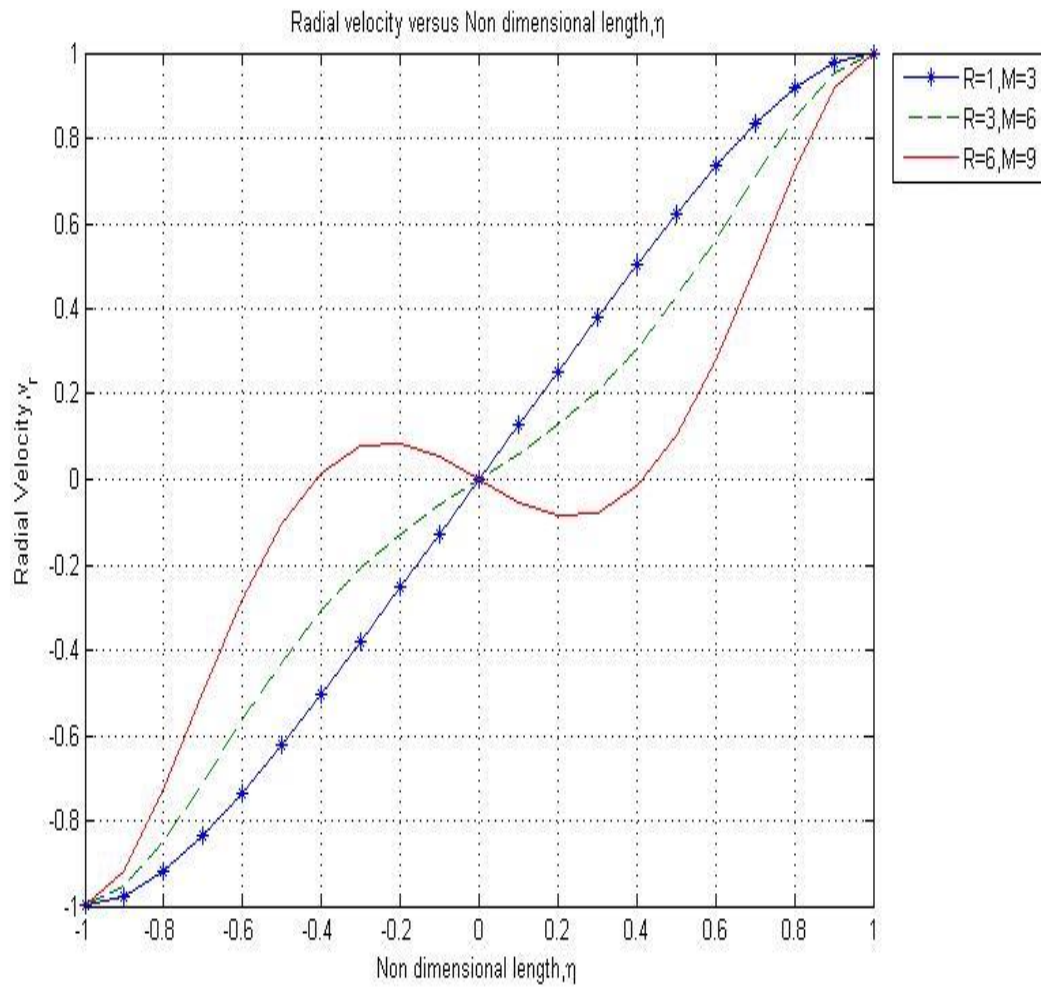


Figure 4.3: Graph of radial velocity profiles as a function of η for the range of $R(1-6)$ and $M(3,6,9)$

In Figure 4.3 as M and R increases tremendously the radial velocity profile steepens for the range $-1 \leq \eta \leq 0$ and reduces in the range $0 \leq \eta \leq 1$. This is because viscous forces are minimal and the flow is dominated by inertia forces and electric conductivity is high.

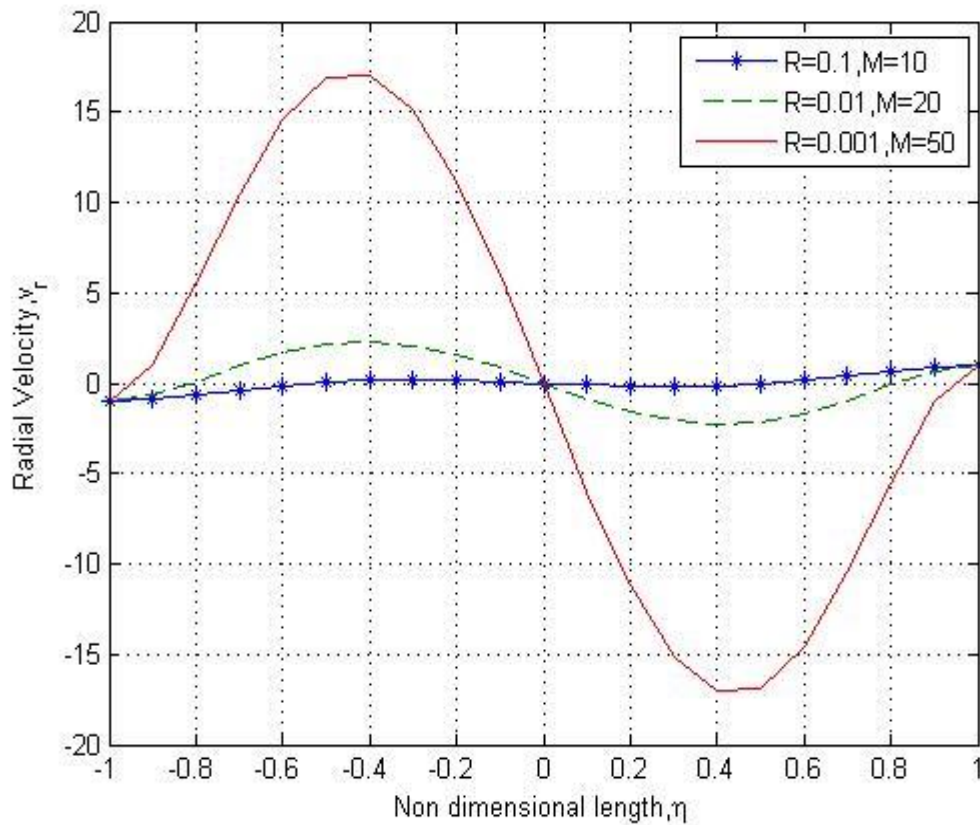


Figure 4.4: Graph of radial velocity profiles as a function of η for small R and large M

In Figure 4.4 as the increase of Reynolds number from 0.1 to 0.001 and as M increases (10 to 50) the radial velocity profile becomes more sinusoidal about the central position and flat near the plates. The curve has a minimum turning point between $0 \leq \eta \leq 1$ due to the high presence of magnetic field which reduces the radial velocity towards the plates.

4.2.2 Axial velocity, v_a

The axial velocity v_a (parallel to x-axis) is the derivative of the radial velocity (parallel to y-axis) given by equation (3.62). The values of the axial velocity, v_a are plotted against

the non dimensional length η and varying the suction Reynolds number, \mathbf{R} and Hartmann, \mathbf{M} as shown by the tables A2, A3 and A4 in appendix A and its corresponding Figures 4.5, 4.6 and 4.7 below.

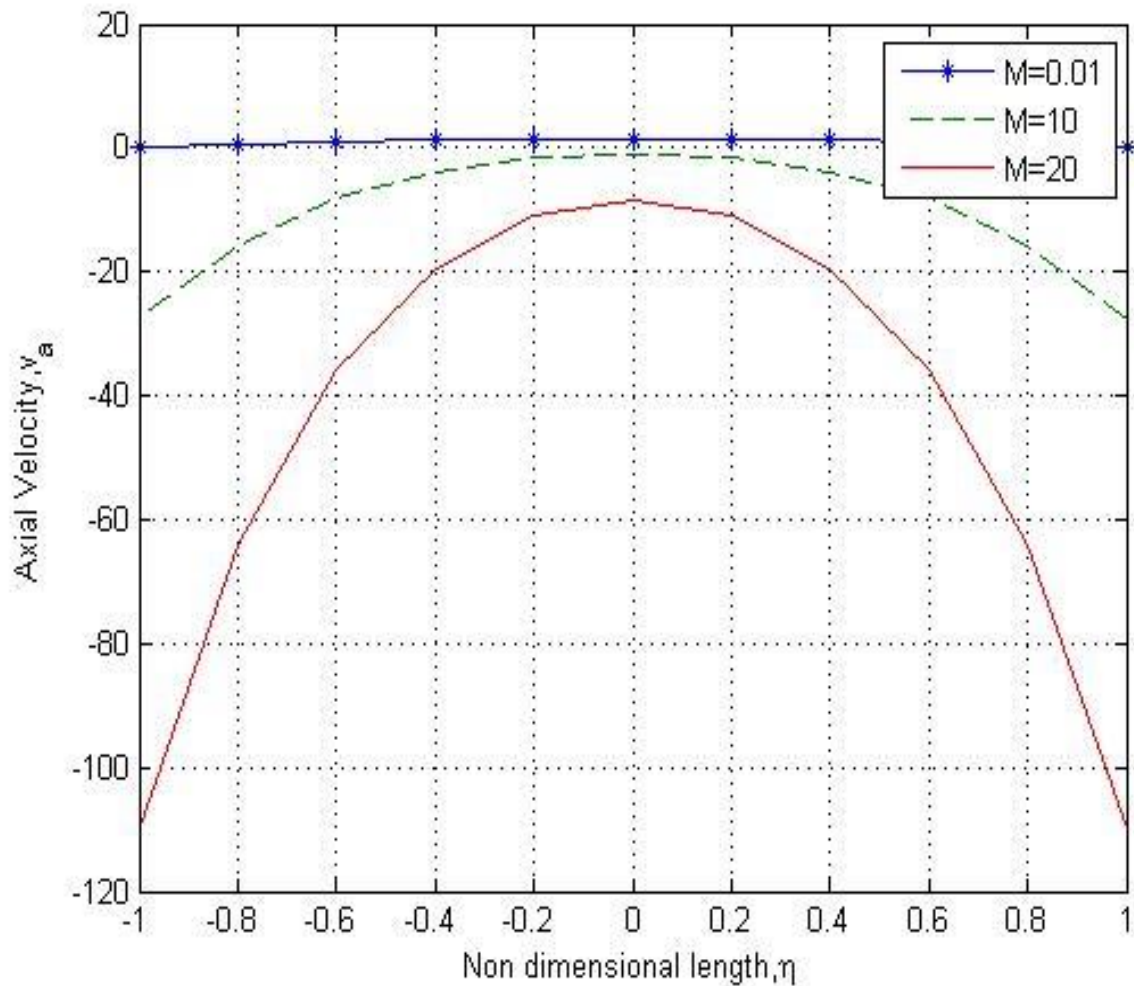


Figure 4.5: Graph of radial velocity profiles as a function of η for constant $R=0.001$ and varying M (0.01, 10, and 20)

In Figure 4.5 it is found that the effect of decreasing M increases velocity field when Reynolds number is kept minimal at 0.001. The fluid velocity profile is parabolic with

maximum magnitude along the channel centerline and minimum at the plates and it stretches outwards as Hartmann number reduces.

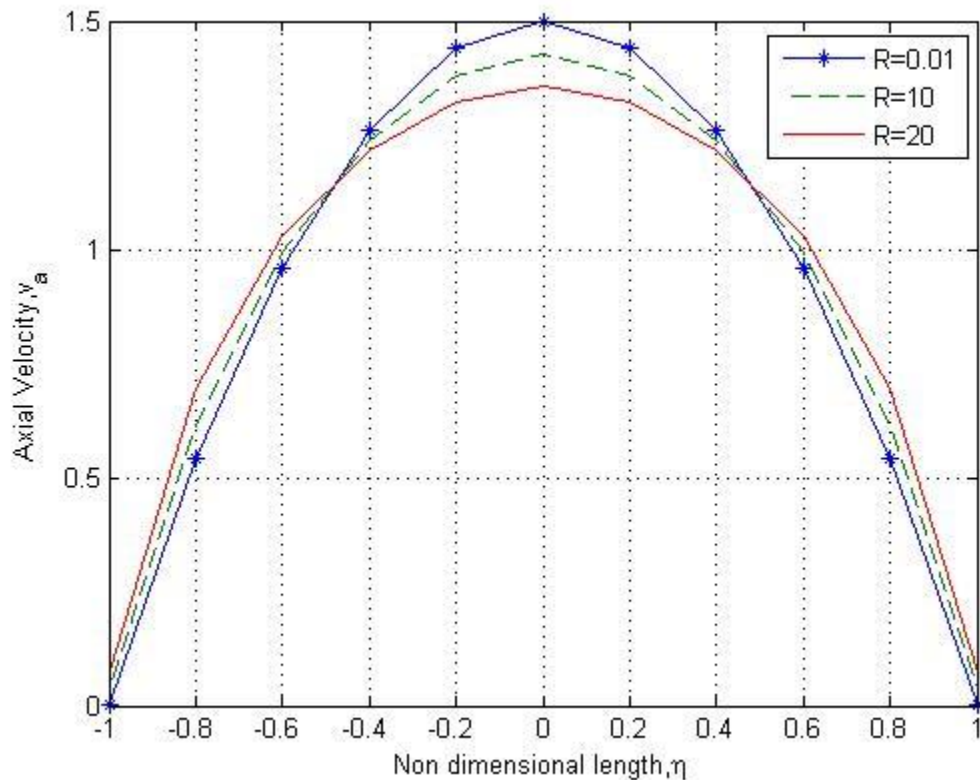


Figure 4.6: Axial velocity profiles as a function of η for Constant $M=0$ and varying R (0.01,10, 20)

Figure 4.6 shows the fluid velocity profile when there is no magnetic field that is when Hartmann number is zero. It is observed that the axial velocity is zero at the plates and increases to the maximum at the central region thus forming a curve with maximum turning point depicting the normal free flow velocity of the stream with very small Reynolds number. As Reynolds number increases the axial velocity decreases meaning that the viscous forces are minimal thus inertia forces dominates the flow.

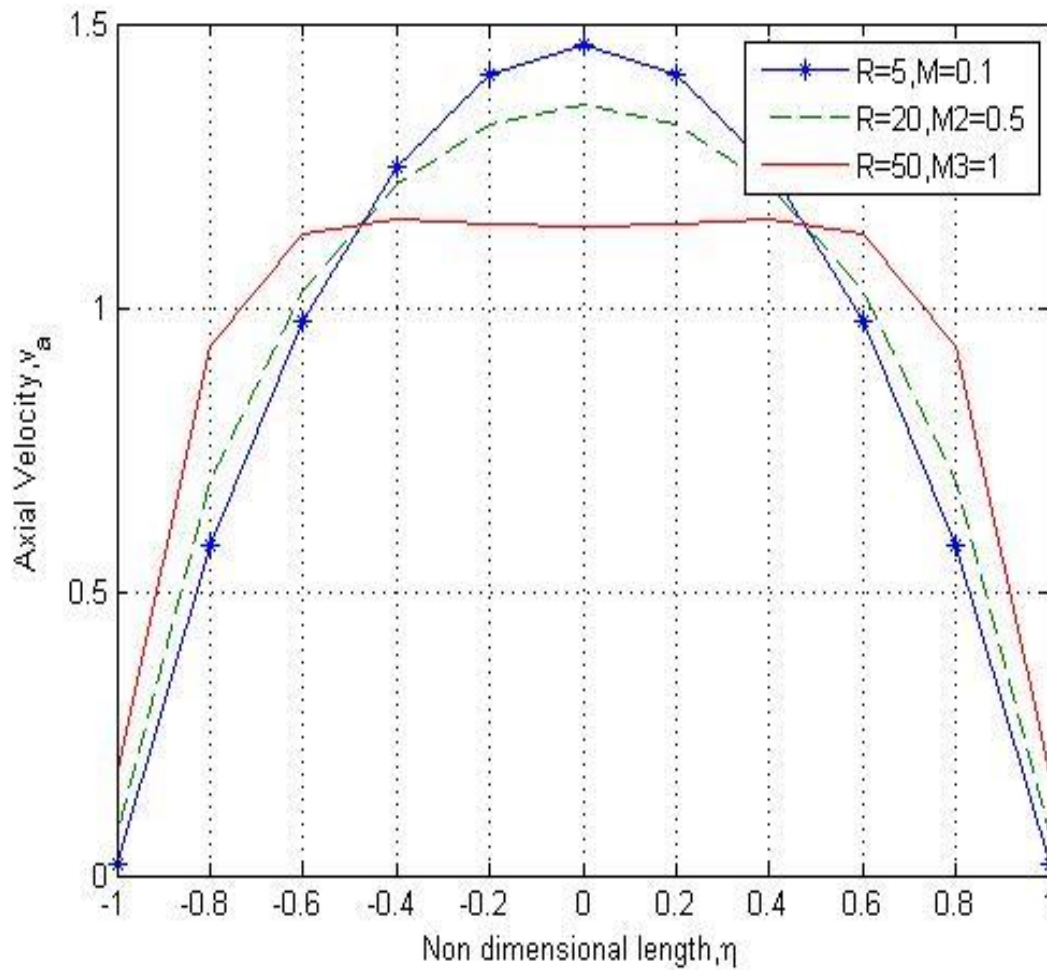


Figure 4.7: Graph of axial velocity profiles as a function of η for large R and small M .

In Figure 4.7, the increase significantly in Reynolds number and insignificantly in Hartmann number reduces the axial velocity. For instance, when $R=50$ and $M=0.1$ there is almost the same velocity in the range -0.6 to 0.6 this indicates that when there is less presence of magnetic field the flow is dominated by inertia forces.

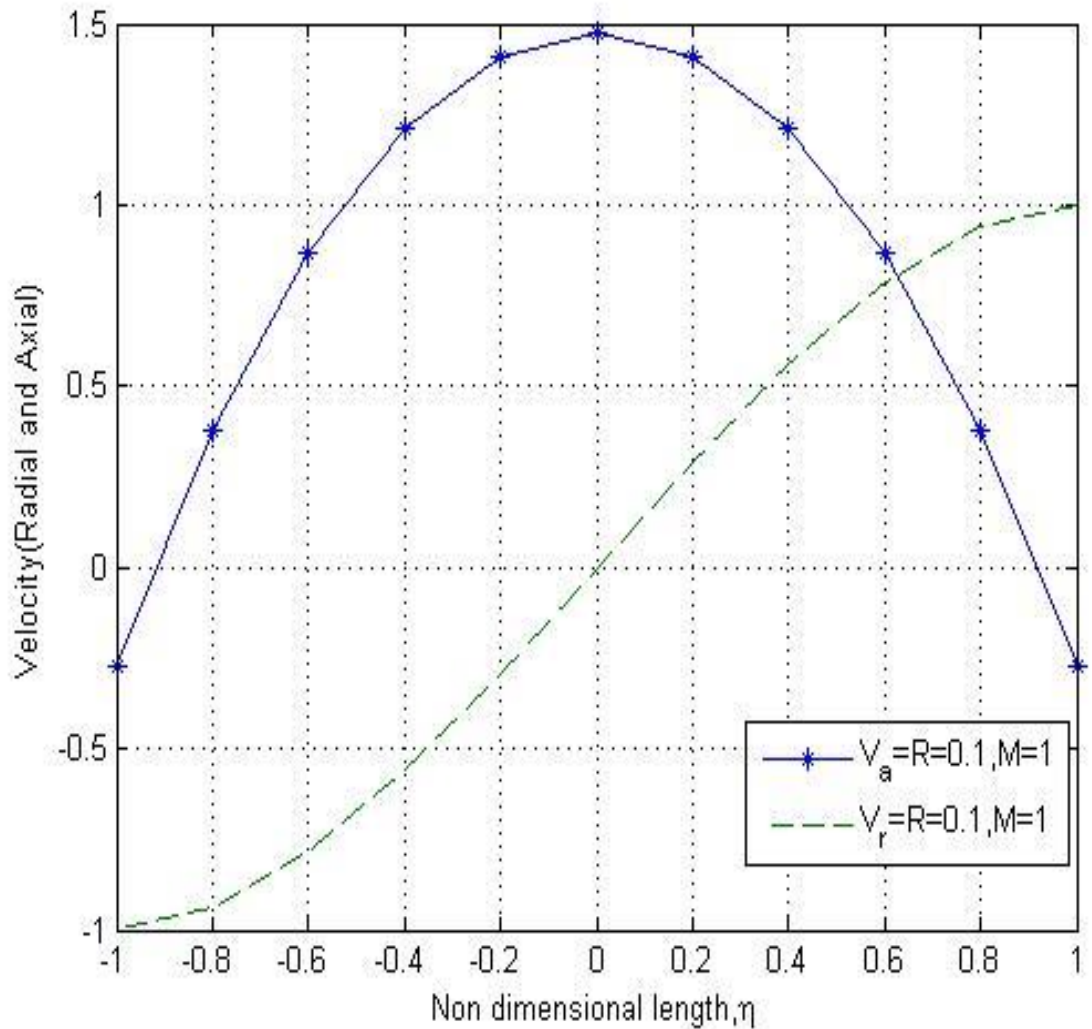


Figure 4.8: Graph of radial and axial velocity profiles as a function of η for $R=0.1$ and $M=1$

Figure 4.8 compares the radial and axial velocities at low Reynolds and Hartmann numbers. It is observed that axial velocity (parallel to x-axis) forms a parabolic curve which shows that the fluid velocity retards at the plates and maximum at the centre of the plates while the radial velocity (parallel to y-axis) increases with increase in non

dimensional length. This indicates the presence of viscous forces and magnetic field in the fluid flow.

4.2.3 Temperature

From the temperature distribution expression (3.30) for the fluid flow, the temperature profile is obtained by plotting the non dimensionless temperature, θ against the non dimensional length, η as depicted by the table 4.5 in the appendix 1 and the graph of figure 4.9 below. The values of Prandtl number and Eckert number are varied.

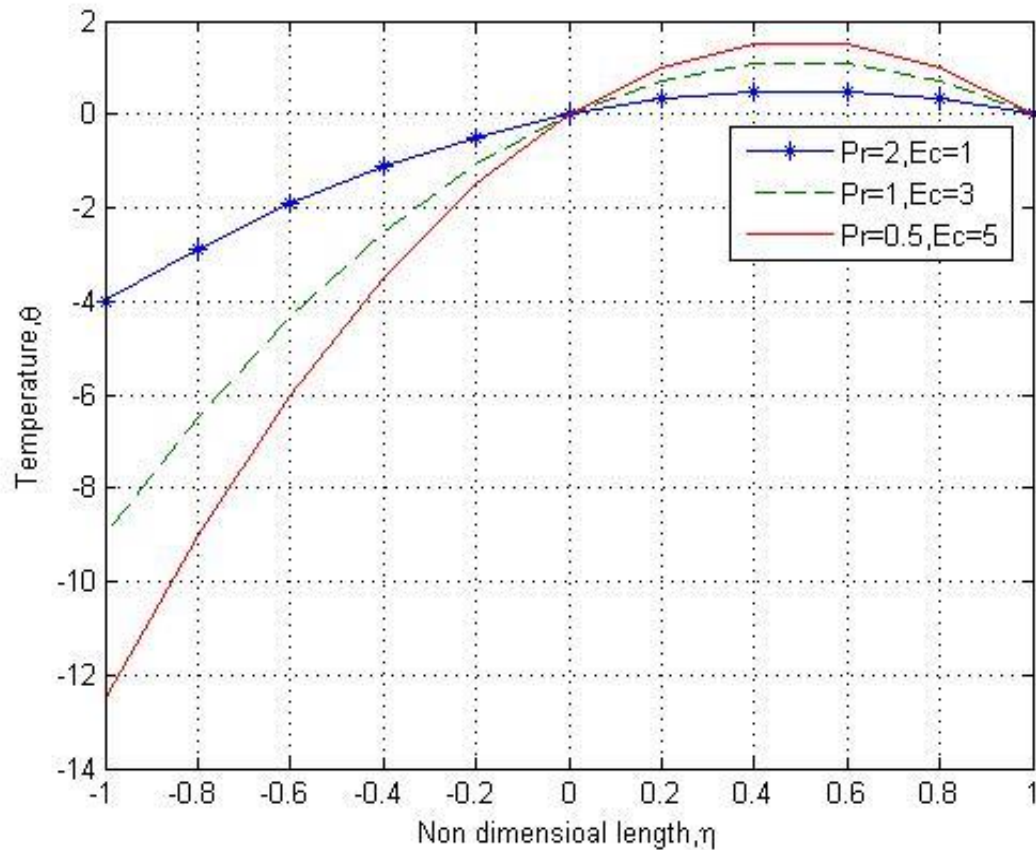


Figure 4.9: Graph of temperature profiles as a function of η for $P_r(2, 1, 0.5)$ and $E_c(1, 3, 5)$

Figure 4.9 shows the temperature profile as a function of the non dimensional length with dimensionless numbers Prandtl and Eckert. It shows that when the Prandtl number increases and Eckert number decreases, the temperature of the fluid decreases. This means that when viscous forces increases in the flow the thermal conductivity becomes negligible and thus thermal energy surpasses the kinetic energy. It is observed that there is a general decrease in the fluid temperature profiles within the channel with increase in Prandtl number. The negative values of temperature can be understood as a reversal of the heat flow that is the temperature gradient at the walls causes a change in the direction of the heat flow and heat transfer does not increase any further.

4.3 Discussion

The Figures 4.1, 4.2, 4.3 and 4.4 discusses the effects of porous plates on the radial velocity (parallel to y-axis). It shows that the radial velocity decreases when Reynolds number increases and Hartman number decreases in the flow. This shows that when the fluid is non MHD ($M=0$) that is no magnetic field existing in the flow the radial velocity reduces. The study of Das et al [2008] which analyzed a three dimensional couette flow of a viscous incompressible electrically conducting fluid between two infinite horizontal parallel porous flat plates in the presence of a transverse magnetic field found that magnetic parameter retards the main fluid velocity and accelerates radial velocity of the flow field which agrees with this study. When there is a decrease in M and increase in Re , the radial velocity profile is less sinusoidal about the centre of the flow as depicted by Figures 4.1 and 4.3 while decrease in Re and increase in M the radial velocity profile becomes more sinusoidal about the central position and flat near the plates as indicated by Figures 4.2 and 4.4.

It is interesting to note that in figures 4.5, 4.6 and 4.7 the fluid velocity decreases with increasing in magnetic field. The fluid velocity profile is parabolic with maximum magnitude along the channel centerline and minimum at the plates and it stretches outwards as Hartmann number reduces. When Hartmann number is zero, the axial velocity is zero at the plates and increases to the maximum at the central region thus forming a curve with maximum turning point depicting the normal free flow velocity of the stream with very small Reynolds number. The axial velocity decreases when Reynolds number increases meaning that the viscous forces are minimal hence inertia forces dominate the flow. Figure 4.8 compares the radial and axial velocities at low Reynolds and Hartmann numbers. It is observed that axial velocity (parallel to x-axis) forms a parabolic curve which shows that the fluid velocity retards at the plates and maximum at the centre of the plates while the radial velocity (parallel to y-axis) increases with increase in non dimensional length. This indicates the presence of viscous forces and magnetic field in the fluid flow.

Figure 4.9 shows that the temperature of the fluid decreases when the Prandtl number increases and Eckert number decreases. An increase in Eckert number leads to an increase in temperature profile, this increase causes the fluid to become warmer and therefore temperature increases due to viscous dissipation which agrees with the study of Okelo [2007].

The negative values of temperature indicates a reversal of the heat flow that is the temperature gradient at the walls causes a change in the direction of the heat flow and heat transfer does not increase any further.

CHAPTER FIVE

CONCLUSION AND RECOMMENDATION

5.1 Conclusion

The solution of the non-linear third order partial differential equation of a steady hydromagnetic flow of a conducting viscous incompressible fluid through a channel with two parallel porous plates was considered. The plates were stationary and a magnetic field transverse at right angle to the electric field. Due to the porous nature of the plates, the fluid was withdrawn through both walls of the channel at the same rate. The specific equations governing the flow were discussed, transformed using dimensionless techniques into a third order partial differential equation which was simplified using Taylor's series expansion and solved by the method of regular perturbation. Expressions for the velocity components and temperature profiles were represented in form of tables and graphs plotted by use of MATLAB programming software. The velocity profiles parallel (axial) and normal (radial) to the plates as well as the temperature distribution on the fluid were investigated.

The effect of porous plates of the hydromagnetic flow on radial velocity and axial velocity indicated that radial velocity decreased with increase in Reynolds number while the axial velocity was zero at the walls and increased to the maximum at the centre line depicting the normal free flow velocity of the stream when there was no magnetic field in the fluid flow. The velocity of the fluid decreased with increase in Hartmann number.

The effect of the dimensionless numbers; Reynolds, Re and Hartmann, M numbers on the flow indicates that when M and Re are significantly small the radial velocity is less

sinusoidal about the centre of the flow and increases as the non dimensional numbers increases. It's also found that the effect of decreasing M increases velocity field when Re number is kept minimal.

The effect of temperature distribution in the fluid shows that when the Prandtl number increases and Eckert number decreases, the temperature of the fluid decreases. This means that when viscous forces increases in the flow the thermal conductivity becomes negligible and thus thermal energy surpasses the kinetic energy. It is also observed that there is a general decrease in the fluid temperature profiles within the channel with increase in Prandtl number. The negative values of temperature can be understood as a reversal of the heat flow that is the temperature gradient at the walls causes a change in the direction of the heat flow and heat transfer does not increase any further.

5.2 Recommendations

The knowledge of this study has importance in solving the problem of constant leakages of oil from the piston-cylinder hydraulic systems where it is assumed that the piston is stationary and the gap width is small hence the flow of oil between two fixed parallel plates. The velocity profiles and temperature profiles found can play a great role in many industrial processes for instance the removal of pollutants from plant discharge stream by absorption and also in MHD devices that utilizes the interaction between velocity profiles, magnetic and electric fields in the design of various machines. It is therefore, recommended that more research studies be done in this exciting field especially when:

- 1) The fluid flow is unsteady
- 2) The boundary plates are inclined at an angle to the horizontal plane
- 3) The porosity of the plates is not uniform on the boundary plates.
- 4) The use of higher order perturbations to improve the accuracy
- 5) The fluid flow is steady with wavy stationary porous plates.

REFERENCES

- Attia, H. A. (1997). Transient MHD Flow and Heat transfer between Two Parallel Plates with Temperature dependent Viscosity. *Mechanic Resource Community* , Vol 26 115-121.
- Baoku I.G, Israel-Cookey and Olajuwon. (2010). Magnetic Field and Thermal radiation effects on Steady Hydromagnetic Couette flow through a porous channel. *Surveys in mathematics and its applications* , Vol. 5 ,215-228.
- Bhargava and Takhar. (2001). Numerical solution of free convection MHD micropolar fluid between two parallel porous vertical plates. . *International Journal of Engineering Science* , Volume 41, Issue 2: pp 123-136.
- Das S. S., Mohanty M., Panda J. P., Sahoo S. K. (2008). Hydromagnetic Three Dimensional Couette flow and Heat transfer. *Journal of Naval Architecture and Marine Engineering* , Vol 5 1-10.
- Das S.S.,Mohanty M and Sahu M. (2012). Finite difference approach on magnetohydrodynamic flow and heat transfer in a viscous incompressible fluid between two parallel porous plates. *International Journal of Energy and Environment* , volume 3, Issue 5, 201.
- Daskalaski, J. (1990). Couette flow through a porous medium of a high Prandtl number fluid with temperature dependent viscosity. *International Journal of Energy Research* , volume 14 21-26.
- Faraday, M. (2016, 26th July, Tuesday at 1900 hrs). Open Library. Org/books/016347m/expermental. *Researches in electricity* .
- Govinda P. R and Jain M. (1966). Hydromagnetic laminar flow through conducting parallel porous plates. *Physical Society of Japan* , pp 1255-1266.
- Govinda P.R. and Jain M. K. (1966). Hydromagnetic Laminar flow through parallel porous plates. *The Physical Society of Japan* , Vol.22,pp 1255-1266.
- Greif R., Habib I.S, and Lin J.C. (1971). Laminar convection of radiating gas in a vertical channel. *Journal of Fluid Mechanics* , 46,513-520.
- Guria, M. (2008). Hydromagnetic flow between two porous disks rotating about non coincidental axes. *Acta Mechanica Sinica* , Volume 24 number 5,489-496.
- Hazeem, A. (2006). Influence of temperature dependents viscosity on . Article ID 75290.

- Israel Cookey and Nwaigwe. (2010). On steady hydromagnetic flow of a radiating viscous fluid through a horizontal channel in a porous medium. *American Journal of Scientific and industrial research*, 1(2) 303-308.
- Kearsley, A. (1994). A steady state model of Couette flow with viscous heating. *International Journal of Engineering science*, 32: 179-186.
- Kimeu B., Kwanza J. and Onyango T. (2014 2(5)). Investigation of hydromagnetic steady flow between two infinite parallel vertical porous plates. *American journal of Applied Mathematics*, 170-178.
- Kumar A, Varshney C. L., Lal S. (2010). Perturbation technique to unsteady periodic flow of viscous fluid through a planar channel. *Journal of engineering Technology Research*, Volume 2(4): 73-81.
- Manyonge W. A, Kiema D.W and Iyaya C. C. (2012). Steady MHD Poiseuille flow between two infinite parallel porous plates in an inclined magnetic field. *International Journal of pure and applied mathematics*, Vol.76, No 5, 661-668.
- Mohanty, A. (2006). *Fluid Mechanics, 2nd Edition*. New Delhi: Prentice-Hall of India Private Limited.
- Murray, S. (1981). *Vector Analysis and an introduction to Tensor Analysis*. Singapore: McGraw-Hill International Book Company.
- Okelo, J. (2008). Heat and Mass transfer past a semi-infinite vertical porous plate in MHD flow. *unpublished thesis*.
- Prasad B.G. and Amit Kumar. (2011). Flow of a Hydromagnetic fluid through porous media between permeable beds under exponentially decaying pressure gradient. *Computational methods in science technology*, Volume 17(1-2) 63-74.
- Ramesh B., Murulidhara N. (Vol 1. 2013). Numerical solution of the MHD Reynolds equation for squeeze-film lubrication between porous and rough rectangular plates. *International journal of Engineering Mathematics*, pp. 933-935.
- Rao, Vdyanidhal V. and Ramana. (1969). Two dimensional unsteady flow of a conducting viscous incompressible fluid between two parallel porous plates. *Proceeding mathematical sciences*, Volume 72 number 6, 272-278.
- Raptis A., Massias C. and Tzivanidis G. (1982). Hydromagnetic free convection flow through a porous medium between two parallel plates. *Physics letters*, 90 (A), pp 288-289.

S, A. (2010). Heat and Mass transfer in MHD Visco-Elastic fluid flow through porous medium over a stretching sheet with chemical reaction. *Journal of Applied Mathematics* , Vol 1 pp. 446-455.

S. N. Aristov and I. M. Gitman. (2002). Viscous flow between two moving parallel disks: exact solutions and stability analysis. *Journal of Fluid Mechanics* , vol. 464, pp. 209–215.

Screenivasulup, Bhaskar M., and Reddy M. (9(7)2013). Effects of radiation on MHD Thermosolutal Marangoni convection boundary layer flow with Joule heating and viscous dissipation. *Journal of Applied mathematics and Mechanics* , pp. 47-65.

Sharma P. R. and Yadav G. R. (2005). Heat Transfer through Three Dimensional Couette flow between a Stationary Porous Plate bounded by porous medium and a moving porous plate. *Utra Science Physicis* , Vol 17(3M) 351-360.

Singh, C. (2014). Hydromagnetic steady flow of liquid between two parallel infinite plates under applied pressure gradient when upper plate is moving with constant velocity under the influence of inclined magnetic field. *Kenya Journal of Science Series A* , Vol. 15, No. 2.

APPENDICES

APPENDIX I: Data for radial velocity, axial velocity and temperature

Table A1: Radial velocity, v_r for $M = 0$ and varying R

η	$R = 0.001$	$R = 50$	$R = 100$
-1	-0.999999999999000	-0.999999950000000	-0.999999900000000
-0.8	-0.943999022445373	-0.895122268648960	-0.846244537297920
-0.6	-0.791997928594205	-0.688429710257280	-0.584859420514560
-0.4	-0.567997822720011	-0.459136000536320	-0.350272001072640
-0.2	-0.295998657097166	-0.228854858285440	-0.161709716570880
0	0	0	0
0.2	0.295998657097166	0.228854858285440	0.161709716570880
0.4	0.567997822720011	0.459136000536320	0.350272001072640
0.6	0.791997928594205	0.688429710257280	0.584859420514560
0.8	0.943999022445373	0.895122268648960	0.846244537297920
1	0.999999999999000	0.999999950000000	0.999999900000000

Table A2: Radial velocity for $R = 0.001$ and varying M

η	$M = 0.01$	$M = 10$	$M = 20$
-1	-0.999999999999000	-0.999999999999000	-0.999999999998998
-0.8	-0.943998763245373	-0.684799022445373	0.092800977554624
-0.6	-0.791997314194205	-0.177597928594205	1.665602071405796
-0.4	-0.567997117120011	0.137602177279989	2.254402177279990
-0.2	-0.295998196297166	0.164801342902834	1.547201342902834
0	0	0	0
0.2	0.295998196297166	-0.164801342902834	-1.547201342902834
0.4	0.567997117120011	-0.137602177279989	-2.254402177279990
0.6	0.791997314194205	0.177597928594205	-1.665602071405796
0.8	0.943998763245373	0.684799022445373	-0.092800977554624
1	0.999999999999000	0.999999999999000	-0.999999999998998

Table A3. Values of Radial velocity when varying both M and R

η	$M = 3$ $R = 1$	$M = 6$ $R = 3$	$M = 9$ $R = 6$
-1	-0.99999999000000	-0.99999997000000	-0.99999994000000
-0.8	-0.919694445372979	-0.847755336118938	-0.728182672237875
-0.6	-0.734632594205146	-0.564601782615437	-0.281907565230874
-0.4	-0.502318720010726	-0.307452160032179	0.016599679935642
-0.2	-0.253185097165709	-0.126083291497126	0.085305417005747
0	0	0	0
0.2	0.253185097165709	0.253185097165709	-0.085305417005747
0.4	0.502318720010726	0.502318720010726	-0.016599679935642
0.6	0.734632594205146	0.734632594205146	0.281907565230874
0.8	0.919694445372979	0.919694445372979	0.728182672237875
1	0.99999999000000	0.99999999000000	0.99999994000000

Table A4: Values of Radial velocity for very small R and large M

η	$M = 10$ $R = 0.1$	$M = 20$ $R = 0.01$	$M = 50$ $R = 0.001$
-1	-0.999999999900000	-0.999999999989999	-0.999999999989991
-0.8	-0.684702244537298	0.092809775546270	5.536000977554622
-0.6	-0.177392859420514	1.665620714057948	14.568002071405797
-0.4	0.137817727998928	2.254421772799892	17.072002177279984
-0.2	0.164934290283429	1.547213429028343	11.224001342902831
0	0	0	0
0.2	-0.164934290283429	-1.547213429028343	-11.224001342902831
0.4	-0.137817727998928	-2.254421772799892	-17.072002177279984
0.6	0.177392859420514	-1.665620714057948	-14.568002071405797
0.8	0.684702244537298	-0.092809775546270	-5.536000977554622
1	0.999999999900000	0.999999999989999	0.999999999989991

Table A5: Axial velocity values for constant $R=0.001$ and varying M

η	$M = 0.01$	$M = 10$	$M = 20$
-1	-0.999999999999000	-0.999999999999000	-0.99999999998998
-0.8	-0.943998763245373	-0.684799022445373	0.092800977554624
-0.6	-0.791997314194205	-0.177597928594205	1.665602071405796
-0.4	-0.567997117120011	0.137602177279989	2.254402177279990
-0.2	-0.295998196297166	0.164801342902834	1.547201342902834
0	0	0	0
0.2	0.295998196297166	-0.164801342902834	-1.547201342902834
0.4	0.567997117120011	-0.137602177279989	-2.254402177279990
0.6	0.791997314194205	0.177597928594205	-1.665602071405796
0.8	0.943998763245373	0.684799022445373	-0.092800977554624
1	0.999999999999000	0.999999999999000	0.99999999998998

Table A6: Axial velocity for values of Constant $M=0$ and varying R (0.01, 10, 20)

η	$R = 0.01$	$R = 10$	$R = 20$
-1	0.000357142400000	0.035714240000000	0.071428480000000
-0.8	0.540078111980973	0.618111980973440	0.696223961946880
-0.6	0.960034287992514	0.994287992514560	1.028575985029120
-0.4	1.259979122283609	1.239122283608960	1.218244567217920
-0.2	1.439941414857713	1.381414857712640	1.322829715425280
0	1.499928571430000	1.428571430000000	1.357142860000000
0.2	1.439941414857713	1.381414857712640	1.322829715425280
0.4	1.259979122283609	1.239122283608960	1.218244567217920
0.6	0.960034287992514	0.994287992514560	1.028575985029120
0.8	0.540078111980973	0.618111980973440	0.696223961946880
1	0.000035714240000	0.035714240000000	0.071428480000000

Table A7: Axial velocity Values for small R and large M

η	$M = 0.001$	$M = 0.5$	$M = 0.1$
	$R = 5$	$R = 20$	$R = 50$
-1	0.017856845000000	0.070740980000000	0.178543700000000
-0.8	0.579055828526720	0.695819061946880	0.930543708867200
-0.6	0.977143904297280	1.028346085029120	1.131430766572800
-0.4	1.249561090244480	1.218115667217920	1.155606262044800
-0.2	1.410707397696320	1.322751815425280	1.147071172563200
0	1.464285690000000	1.357080360000000	1.142854650000000
0.2	1.410707397696320	1.322751815425280	1.147071172563200
0.4	1.249561090244480	1.218115667217920	1.155606262044800
0.6	0.977143904297280	1.028346085029120	1.131430766572800
0.8	0.579055828526720	0.695819061946880	0.930543708867200
1	0.017856845000000	0.070740980000000	0.178543700000000

Table A8: Comparison of Radial and Axial velocities

η	v_r $M = 1$ $R = 0.1$	v_a $M = 1$ $R = 0.1$
-1	-0.274642857600000	-0.999999999900000
-0.8	0.378821119809734	-0.941310244537298
-0.6	0.868382879925146	-0.785648859420515
-0.4	1.208231222836090	-0.560726272001072
-0.2	1.408254148577127	-0.291257709716571
0	1.474285714300000	0
0.2	1.408254148577127	0.291257709716571
0.4	1.208231222836090	0.560726272001072
0.6	0.868382879925146	0.7856sss48859420515
0.8	0.378821119809734	0.941310244537298
1	-0.274642857600000	0.999999999900000

Table A9: Temperature Values for $P_r(2, 1, 0.5)$ and $E_c(1, 3, 0.5)$

η	$Pr = 2$ $E_c = 1$	$Pr = 1$ $E_c = 3$	$Pr = 0.5$ $E_c = 0.5$
-1	-4.000000000000000	-9.000000000000000	-1.250000000000000
-0.8	-2.880000000000000	-6.480000000000001	-0.900000000000000
-0.6	-1.920000000000000	-4.319999999999999	-0.600000000000000
-0.4	-1.120000000000000	-2.519999999999999	-0.350000000000000
-0.2	-0.480000000000000	-1.080000000000000	-0.150000000000000
0	0	0	0
0.2	0.320000000000000	0.720000000000000	0.100000000000000
0.4	0.480000000000000	1.080000000000000	0.150000000000000
0.6	0.480000000000000	1.080000000000000	0.150000000000000
0.8	0.320000000000000	0.720000000000000	0.100000000000000
1	0	0	0

APPENDIX II: MATLAB Program

Program 1 for Figure 4.1

```

format long

n=-1:0.2:1;

m=0;

R1=0.001;

y1=0.5*n.*(3-n.^2)+0.010714285*R1*n.^3-0.003571429*R1*n.^7-0.025*m^2*n.^5-
0.025*m^2*n-0.007142857*R1*n+0.05*m^2*n.^3

R2=50;

y2=0.5*n.*(3-n.^2)+0.010714285*R2*n.^3-0.003571429*R2*n.^7-0.025*m^2*n.^5-
0.025*m^2*n-0.007142857*R2*n+0.05*m^2*n.^3

R3=100;

y3=0.5*n.*(3-n.^2)+0.010714285*R3*n.^3-0.003571429*R3*n.^7-0.025*m^2*n.^5-
0.025*m^2*n-0.007142857*R3*n+0.05*m^2*n.^3

plot(n,y1 , '*-',n,y2,'--',n,y3,'-')

legend('R=0.001','R=50','R=100')

grid on

xlabel('Non dimensiona length,\eta')

ylabel('Radial Velocity,v_r')

```

Program 2 for Figure 4.2

```

format long

n=-1:0.1:1;

m1=0.01;

R1=0.001;

y1=0.5*n.*(3-n.^2)+0.010714285*R1*n.^3-0.003571429*R1*n.^7-0.025*m1^2*n.^5-
0.025*m1^2*n-0.007142857*R1*n+0.05*m1^2*n.^3

R2=0.001;

m2=10;

y2=0.5*n.*(3-n.^2)+0.010714285*R2*n.^3-0.003571429*R2*n.^7-0.025*m2^2*n.^5-
0.025*m2^2*n-0.007142857*R2*n+0.05*m2^2*n.^3

m3=20;

R3=0.001;

y3=0.5*n.*(3-n.^2)+0.010714285*R3*n.^3-0.003571429*R3*n.^7-0.025*m3^2*n.^5-
0.025*m3^2*n-0.007142857*R3*n+0.05*m3^2*n.^3

plot(n,y1 , '*-',n,y2,'--',n,y3,'-')

legend('M=0.01','M=10','M=20')

grid on

xlabel('Non dimensionl lenght, \eta')

ylabel('Radial Velocity,v_r')

```

Program 3 for Figure 4.3

```

format long

n=-1:0.2:1;

m1=3;

R1=1;

y1=0.5*n.*(3-n.^2)+0.010714285*R1*n.^3-0.003571429*R1*n.^7-0.025*m1^2*n.^5-
0.025*m1^2*n-0.007142857*R1*n+0.05*m1^2*n.^3

R2=3;

m2=6;

y2=0.5*n.*(3-n.^2)+0.010714285*R2*n.^3-0.003571429*R2*n.^7-0.025*m2^2*n.^5-
0.025*m2^2*n-0.007142857*R2*n+0.05*m2^2*n.^3

m3=9;

R3=6;

y3=0.5*n.*(3-n.^2)+0.010714285*R3*n.^3-0.003571429*R3*n.^7-0.025*m3^2*n.^5-
0.025*m3^2*n-0.007142857*R3*n+0.05*m3^2*n.^3

plot(n,y1 , '*-',n,y2,'--',n,y3,'-')

legend('R=1,M=3','R=3,M=6','R=6,M=9')

grid on

xlabel('Non dimensional length,\eta')

ylabel('Radial Velocity,v_r')

```

Program 4 for Figure 4.4

```

format long

n=-1:0.1:1;

m1=10;

R1=0.1;

y1=0.5*n.*(3-n.^2)+0.010714285*R1*n.^3-0.003571429*R1*n.^7-0.025*m1^2*n.^5-
0.025*m1^2*n-0.007142857*R1*n+0.05*m1^2*n.^3

R2=0.01;

m2=20;

y2=0.5*n.*(3-n.^2)+0.010714285*R2*n.^3-0.003571429*R2*n.^7-0.025*m2^2*n.^5-
0.025*m2^2*n-0.007142857*R2*n+0.05*m2^2*n.^3

m3=50;

R3=0.001;

y3=0.5*n.*(3-n.^2)+0.010714285*R3*n.^3-0.003571429*R3*n.^7-0.025*m3^2*n.^5-
0.025*m3^2*n-0.007142857*R3*n+0.05*m3^2*n.^3

plot(n,y1 , '*-',n,y2,'--',n,y3,'-')

legend('R=0.1,M=10','R=0.01,M=20','R=0.001,M=50')

grid on

xlabel('Non dimensional length,\eta')

ylabel('Radial Velocity,v_r')

```

Program 5 for Figure 4.5

```

format long

n=-1:0.2:1;

R1=0.001;

m1=0.01;

y1=1.5*(1-n.^2)+0.032142855*R1*n.^2-0.021428574*R1*n.^6-0.1*m1^2*n.^4-
0.025*m1^2-0.007142857*R1-0.15*m1^2*n.^2

R2=0.001;

m2=10;

y2=1.5*(1-n.^2)+0.032142855*R2*n.^2-0.021428574*R2*n.^6-0.1*m2^2*n.^4-
0.025*m2^2-0.007142857*R2-0.15*m2^2*n.^2

R3=0.001;

m3=20;

y3=1.5*(1-n.^2)+0.032142855*R3*n.^2-0.021428574*R3*n.^6-0.1*m3^2*n.^4-
0.025*m3^2-0.007142857*R3-0.15*m3^2*n.^2

plot(n,y1 , '*-',n,y2,'--',n,y3,'-')

legend('M=0.01', 'M=10', 'M=20')

grid on

xlabel('Non dimensional length,\eta')

ylabel('Axial Velocity,v_a')

```

Program 6 for Figure 4.6

```

format long

n=-1:0.2:1;

R1=0.01;

m=0;

y1=1.5*(1-n.^2)+0.032142855*R1*n.^2-0.021428574*R1*n.^6-0.1*m^2*n.^4-
0.025*m^2-0.007142857*R1-0.15*m^2*n.^2

R2=10;

m=0;

y2=1.5*(1-n.^2)+0.032142855*R2*n.^2-0.021428574*R2*n.^6-0.1*m^2*n.^4-
0.025*m^2-0.007142857*R2-0.15*m^2*n.^2

R3=20;

m=0;

y3=1.5*(1-n.^2)+0.032142855*R3*n.^2-0.021428574*R3*n.^6-0.1*m^2*n.^4-
0.025*m^2-0.007142857*R3-0.15*m^2*n.^2

plot(n,y1 , '*-',n,y2,'--',n,y3,'-')

legend('R1=0.01','R2=10','R3=20')

grid on

xlabel('Non dimensional,\eta')

ylabel('Axial Velocity,V_a')

```

Program 7 for Figure 4.7

```

format long

n=-1:0.2:1;

R1=5;

m1=0;

y1=1.5*(1-n.^2)+0.032142855*R1*n.^2-0.021428574*R1*n.^6-0.1*m1^2*n.^4-
0.025*m1^2-0.007142857*R1-0.15*m1^2*n.^2

R2=20;

m2=0;

y2=1.5*(1-n.^2)+0.032142855*R2*n.^2-0.021428574*R2*n.^6-0.1*m2^2*n.^4-
0.025*m2^2-0.007142857*R2-0.15*m2^2*n.^2

R3=50;

m3=0;

y3=1.5*(1-n.^2)+0.032142855*R3*n.^2-0.021428574*R3*n.^6-0.1*m3^2*n.^4-
0.025*m3^2-0.007142857*R3-0.15*m3^2*n.^2

plot(n,y1 , '*-',n,y2,'--',n,y3,'-')

legend('R=5,M=0.1','R=20,M2=0.5','R=50,M3=1')

grid on

xlabel('Non dimensional length,\eta')

ylabel('Axial Velocity,v_a')

```

Program 8 for Figure 4.8

```

format long

n=-1:0.1:1;

R1=10;

m1=0;

y1=1.5*(1-n.^2)+0.032142855*R1*n.^2-0.021428574*R1*n.^6-0.1*m1^2*n.^4-
0.025*m1^2-0.007142857*R1-0.15*m1^2*n.^2

format long

n=-1:0.1:1;

m2=0;

R2=10;

y2=0.5*n.*(3-n.^2)+0.010714285*R2*n.^3-0.003571429*R2*n.^7-0.025*m2^2*n.^5-
0.025*m2^2*n-0.007142857*R2*n+0.05*m2^2*n.^3

plot(n,y1 , '*-',n,y2,'--')

legend('V_a=R=0.1,M=1','V_r=R=0.1,M=1')

grid on

xlabel('Non dimensional length,\eta')

ylabel('Velocity(Radial and Axial)')

title('velocities of radial and axial versus Non dimensional length,\eta')

```

Program 9 for Figure 4.9

```
format long
n=-1:0.2:1;
Pr1=2;
Ec1=1;
y1=n.*(1+0.5*Pr1)*Ec1.*(1-n)
Pr2=1;
Ec2=3;
y2=n.*(1+0.5*Pr2)*Ec2.*(1-n)
Pr3=0.5;
Ec3=5;
y3=n.*(1+0.5*Pr3)*Ec3.*(1-n)
plot(n,y1 , '*-',n,y2,'--',n,y3,'-')
legend('Pr=2,Ec=1','Pr=1,Ec=3','Pr=0.5,Ec=5')
grid on
xlabel('Non dimensionioal length,\eta')
ylabel('Temperature,\theta')
```